CAMS Service Evolution

D9.1 Intercomparison and evaluation from different angles of the regional and global model, building on the 2022 CAMS2_40 regional model intercomparison

Due date of deliverable	30/6/2025
Submission date	30/6/2025
File Name	CAMAERA-D9.1-v1.0.docx
Work Package /Task	WP9
Organisation Responsible of Deliverable	IOS-PIB/HYGEOS
Author name(s)	Jacek Kaminski/Joanna Struzewska/Samuel Remy/Rose-Cloé Meyer
Revision number	1.0
Status	
Dissemination Level	PU

The CAMAERA project (grant agreement No 101134927) is funded by the European Union.
Views and opinions expressed are however those of the author(s) only and do not necessarily reflect those of the European Union or the Commission. Neither the European Union nor the granting authority can be held responsible for them.

1 Executive Summary

An intercomparison of regional CAMS model has been carried out as part of the CAMS_40 project, focusing on deposition and surface concentration. In this task, our objective is to expand this intercomparison, by integrating new regional models as well as the global CAMS system, and by extending the verification protocol. Two new regional models (GEMS-AQ and MINNI) have been integrated into the regional models intercompared. The global CAMS system (IFS-COMPO) has been run using a similar resolution and using similar emissions as the regional systems. This required the production of an emissions dataset that merged the global and regional components. Running IFS-COMPO at a very high resolution (0.1x0.1°) yielded a lot of information on the impact of dramatically increase the resolution on simulated fields. The intercomparison between the regional models and IFS-COMPO, and evaluation versus observations focused on PM2.5 and PM10. A wealth of results have been produced, which will help in better understanding the behaviour of the regional and global CAMS systems.

Table of Contents

Table des matières

Introduction

2.1 Background

The European Union's flagship Space programme Copernicus provides a key service to the European society, turning investments in space-infrastructure into high-quality information products. The Copernicus Atmosphere Monitoring Service (CAMS, https://atmosphere.copernicus.eu) exploits the information content of Earth-Observation data to monitor the composition of the atmosphere. By combining satellite observations with numerical modelling by means of data assimilation and inversion techniques, CAMS provides in near-real time a wealth of information to answer questions related to air quality, climate change and air pollution and its mitigation, energy, agriculture, etc. CAMS provides both global atmospheric composition products, using the Integrated Forecasting System (IFS) of ECMWF - hereafter denoted the global production system -, and regional European products, provided by an ensemble of eleven regional models - the regional production system.

The CAMS AERosol Advancement (CAMAERA) project will provide strong improvements of the aerosol modelling capabilities of the regional and global systems, on the assimilation of new sources of data, and on a better representation of secondary aerosols and their precursor gases. In this way CAMAERA will enhance the quality of key products of the CAMS service and therefore help CAMS to better respond to user needs such as air pollutant monitoring, along with the fulfilment of sustainable development goals. To achieve this purpose CAMAERA will develop new prototype service elements of CAMS, beyond the current state-of-art. It will do so in very close collaboration with the CAMS service providers, as well as other tier-3 projects. In particular CAMAERA will complement research topics addressed in CAMEO, which focuses on the preparation for novel satellite data, improvements of the data assimilation and inversion capabilities of the CAMS production system, and the provision of uncertainty information of CAMS products.

2.2 Scope of this deliverable

2.2.1 Objectives of this deliverables

This deliverable shows an intercomparison and evaluation of the global and regional CAMS systems. The global CAMS systems has been adapted to use the same emissions over Europe as the regional CAMS models, and has been run at a similar resolution (0.1x0.1°).

Work performed in this deliverable

In this deliverable the work as planned in the Description of Action (DoA, WP9 T9.1) was performed.

3.1 Deviations and counter measures

No deviations have been encountered.

3.2 CAMAERA Project Partners:

HYGEOS	HYGEOS SARL
ECMWF	EUROPEAN CENTRE FOR MEDIUM-RANGE WEATHER FORECASTS
Met Norway	METEOROLOGISK INSTITUTT
RC.io	RESEARCHCONCEPTS IO
BSC	BARCELONA SUPERCOMPUTING CENTER-CENTRO NACIONAL DE SUPERCOMPUTACION
KNMI	KONINKLIJK NEDERLANDS METEOROLOGISCH INSTITUUT-KNMi
SMHI	SVERIGES METEOROLOGISKA OCH HYDROLOGISKA INSTITUT
FMI	ILMATIETEEN LAITOS
MF	METEO-FRANCE
TNO	NEDERLANDSE ORGANISATIE VOOR TOEGEPAST NATUURWETENSCHAPPELIJK ONDERZOEK TNO
INERIS	INSTITUT NATIONAL DE L ENVIRONNEMENT INDUSTRIEL ET DES RISQUES - INERIS
IOS-PIB	INSTYTUT OCHRONY SRODOWISKA - PANSTWOWY INSTYTUT BADAWCZY
FZJ	FORSCHUNGSZENTRUM JULICH GMBH
AU	AARHUS UNIVERSITET
ENEA	AGENZIA NAZIONALE PER LE NUOVE TECNOLOGIE, L'ENERGIA E LO SVILUPPO ECONOMICO SOSTENIBILE

Merging regional and global emissions datasets

In this part, we focus on the global model. The goal is to study the impact of using the regional emissions on Europe in IFS-COMPO. For this, the regional emissions data representing regional emissions must be integrated into the files used in the global model. Then, the simulated fields obtained with the two sets of emissions have been compared and evaluated. We have also studied two configurations with different spatial resolutions.We focus on the year 2018 with meteorological and chemical forcing from IFS-COMPO every three hours.

4.1 Methodology and resulting emissions

In order to run the global system with emissions that are comparable to those of the regional systems, it is necessary to merge the regional emissions into the global files used in IFS-COMPO. However, the data format used in the regional emissions is quite different than in the global emission files. The regional emissions have been merged in the global emissions files for the following species: methane, carbon monoxide, ammonia, non-methane vocs, nitrogen oxides, sulphur dioxide, sulfate, organic carbon and black carbon.

The global emission files are netcdf or grib mensual files, with 36 species distributed in 21 sectors at a resolution of 0.1x0.1. On the other hand, the regional emissions are annual csv files, with 8 initial parameters distributed in 12 sectors, using country by country PM split and a 0.1x0.05 resolution.

First, the different parameters are computed from the regional files using the PM split and the area of each country.

Next, the data are distributed in the sectors. As the regional and global sectors do not overlap perfectly, we had to choose to put certain contributions in one sector or another. For example, all the emissions from the regional sector B_Industry have been supposed to be part of the global sector industrial process, and the emissions for the global sector refineries have been set to zero. The match between the regional and the global sectors, and the hypothesis made on the division of the sectors are detailed in the following table.

Table 2.1. mapping of regional and global emission sectors.

Regional sectors	**Global sectors**
A_PublicPower	Power generation (ene)
B_Industry	~~Refineries (ref) +~~ Industrial process (ind)
C_OtherStationaryComb	~~Commercial (com) +~~ Residential (res)
D_Fugitives	Fugitives (fef)
E_Solvents	Solvents (slv)
F_RoadTransport_exhaust_gasoline :F1,F2,F3,F4	Road transportation (tro)
G_Shipping	Ships (shp)
H_Aviation	Off Road transportation (tnr)
I_OffRoad	Off Road transportation (tnr)
J_Waste	Solid waste and waste water (swd) ~~+ Solid waste landfills (swl)~~
K_AgriLivestock	Agriculture livestock (agl)
L_AgriOther	~~Agriculture soils (ags) +~~ Agricultural waste burning (awb)

Then, the regional data are interpolated to correspond to the longitude and latitude used in the global emission files.

Finally, as the global emissions are monthly while the regional emissions are provided as yearly values, we have to create a seasonal cycle for the regional emission. For this, at each point, the global emissions are averaged and the deviation from the average is computed for each month. Then, the regional annual value is multiplied by the ratio of the monthly global value and the average at this point. With that, the regional emissions in Europe and the global emissions have the same format and can be merged.

We obtain two sets of emissions:

- regional emissions over Europe (CAMS-REG-v5.1 REF2 v2.0.1) and global emissions elsewhere (CAMS_GLOB_ANTv6.1).
- global emissions (CAMS_GLOB_ANTv6.1) everywhere.

In the following, we refer to the two configurations as the “regional emissions” case and the “global emissions” case respectively.

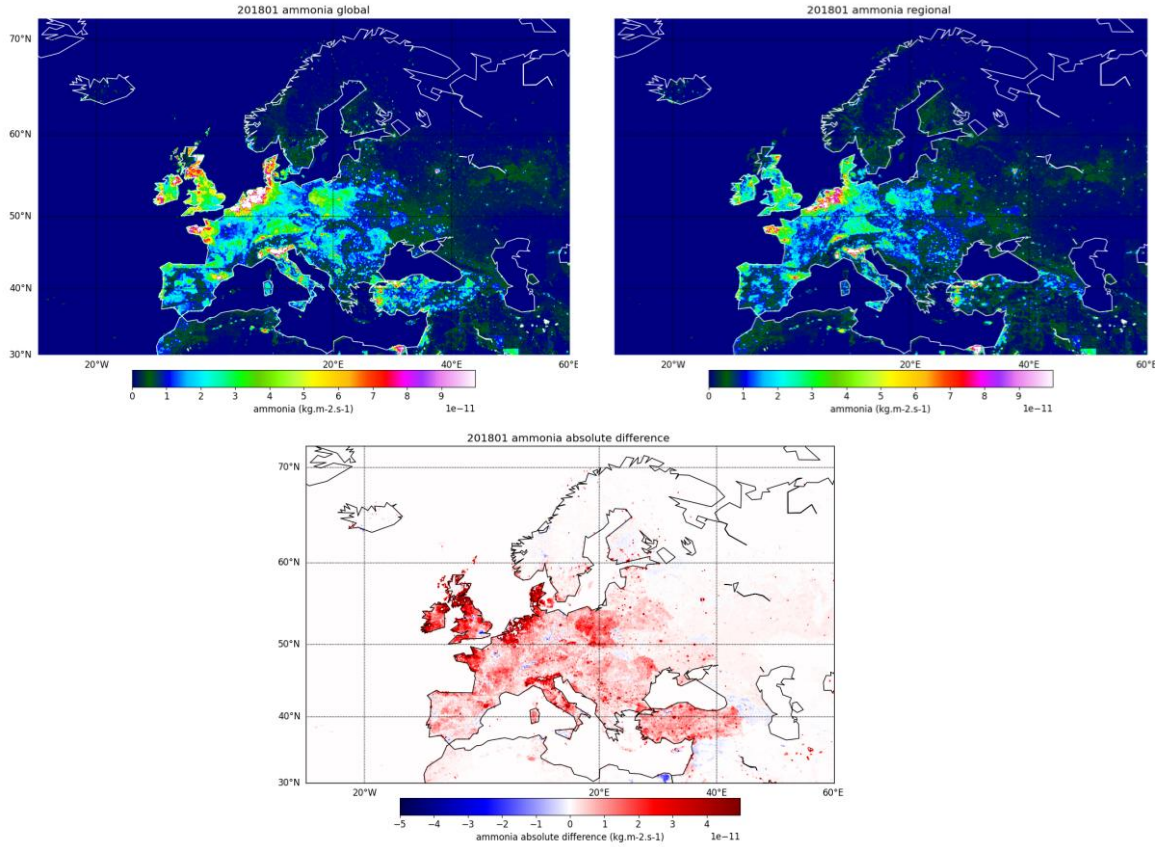

Figure 2.1: Global and regional emissions of ammonia for January 2018

Figure 2.2 show the emissions of organic carbon from the global and regional emissions; the regional totals are much higher because the condensable fraction is included, which is not the case in global emissions.

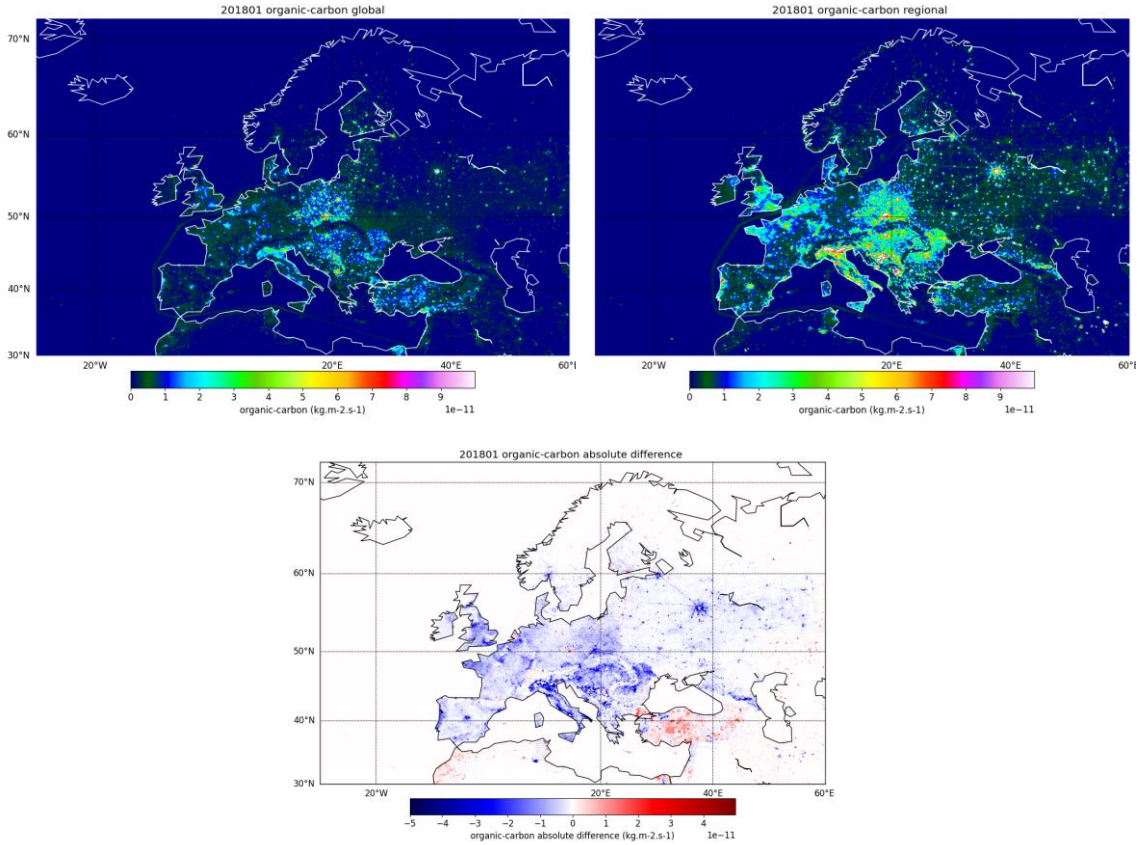

Figure 2.2: Global and regional emissions of organic carbon for January 2018

4.2 Use in IFS-COMPO and evaluation

The emissions dataset that merges global and regional emissions has been used in two forecast (ie without data assimilation) only IFS-COMPO simulations using cycle 49R1, at a low (T_L511, 40 km grid cell) and high (T_{CO}1279 , 9km grid cell) resolution, and compared against similar simulations using the global emissions dataset. The year 2018 has been simulated, in order to follow the task 4042 model intercomparison protocol. In this subsection, only results with low resolution are shown; results with higher resolution are shown in section 3.3 and 4. Figure 2.3 show simulated AOD at 500 and 1020nm versus AERONET observations over Europe. The simulation using regional emissions over Europe show mostly higher values in wintertime, probably mostly from the higher OC emissions in the regional emissions dataset, and lower values during the rest of the year, arising from lower emissions of SO_2 and NH_3 and others in the regional emissions dataset.

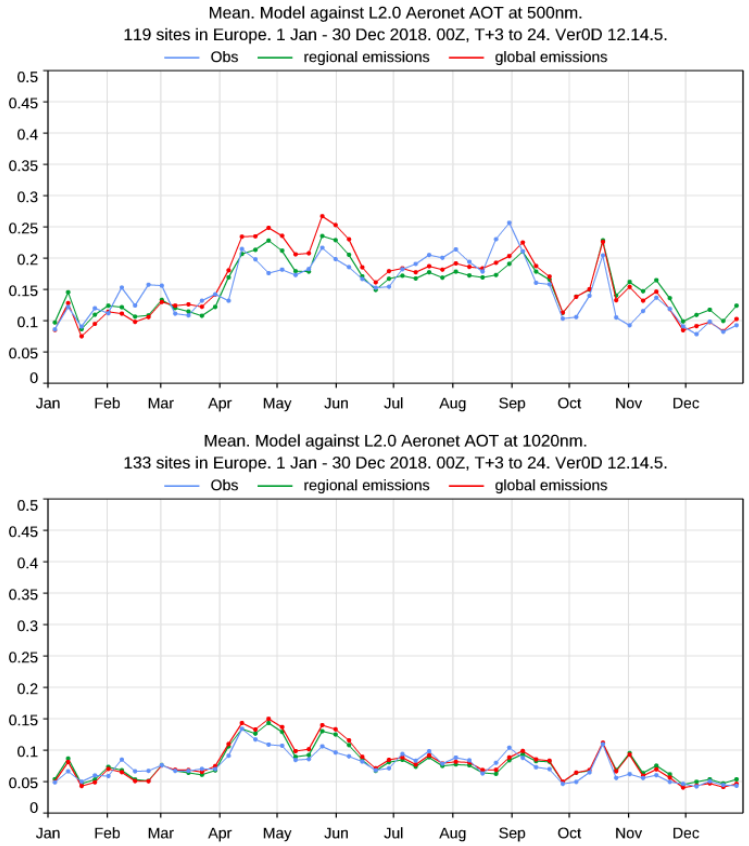

Figure 2.3: Evaluations of simulated weekly AOD against AERONET observations at 550 and 1020 nm over Europe.

Figure 2.4 compares the simulated PM2.5 and PM10 over background rural stations in 2018. The signal of the emissions changes is stronger than for AOD, with a much higher simulated PM2.5 and PM10 in wintertime with the regional emissions, which reduces a significant low bias then, and values that are quite close for the rest of the year.

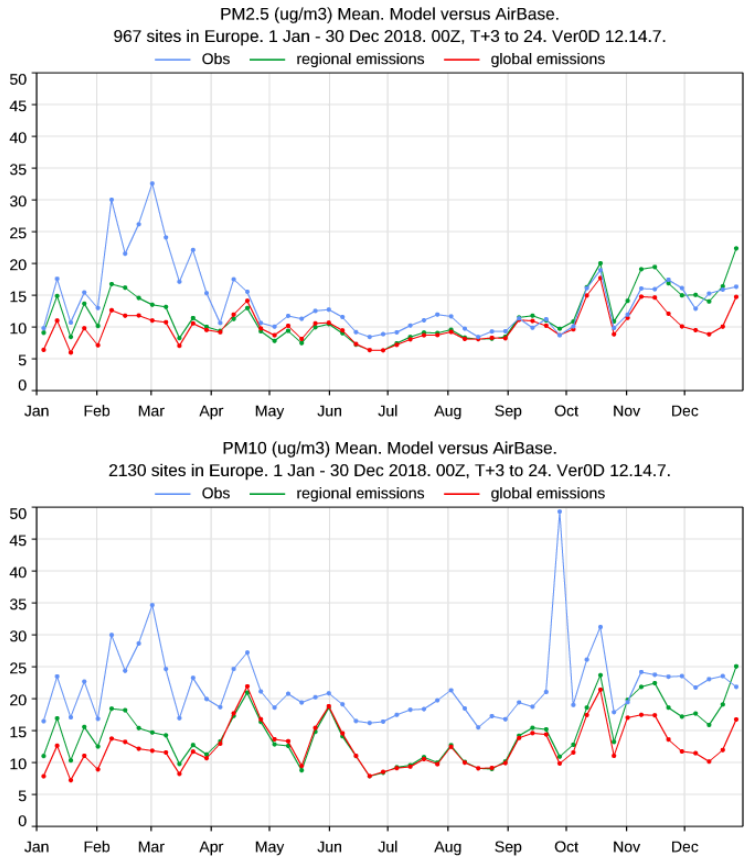

Figure 2.4 : Evaluations of simulated weekly PM2.5 and PM10 against observations from background rural stations from EEA/Airbase.

Figure 2.5 shows the impact of using the regional emissions dataset in IFS-COMPO for a selection of trace gases. Surface NO_2 shows significantly higher simulated values all year long with the regional dataset, which brings the simulated values closer to observed values. Surface ozone and SO_2 on the other hand show lower values, particularly in wintertime. For surface ozone, the impact is clearly positive. Finally, the impact on simulated surface CO is very small in general.

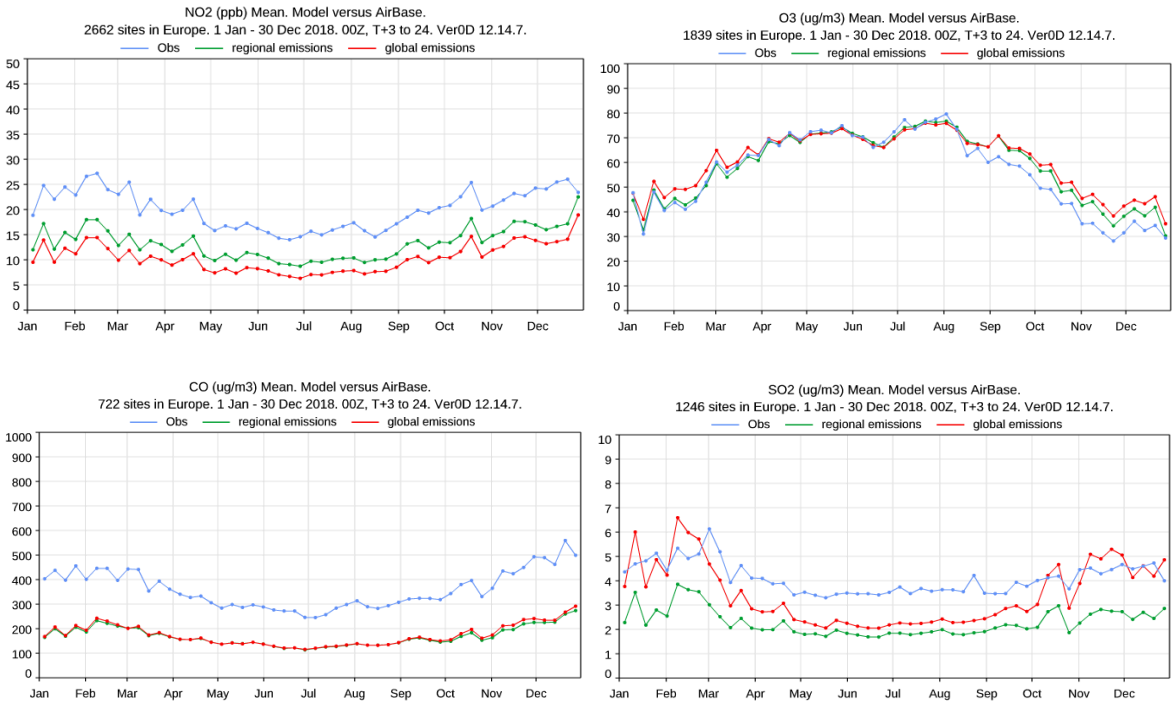

Figure 2.5 : Evaluations of simulated weekly NO_2, O_3, CO, SO_2 against EEA/Airbase observations.

4.3 High resolution IFS-COMPO simulations

In order to compare fields and diagnostics with regional models we need to use similar resolution. For this, high resolution IFS-COMPO runs are carried out with cycle 49R1, at a $T_{CO}1279$ resolution (approx. 9km grid cell), without data assimilation, for the year 2018, in order to follow the protocol of the task 4042 model intercomparison. In addition to the field comparison and diagnostics with the regional models, these experiments are also used to assess the impact of a large resolution upgrade on simulated fields and on the skill of the forecasts. The experiments shown here use the global emissions and not the merged global-regional emissions described in the preceding section. Forecast only simulations with cycle 49R1 at $T_{CO}1279$ using the merged global-regional emissions dataset have also been carried out and are evaluated in section 4.

Two experiments at high resolution have been launched, using regional or global emissions over Europe. Here we focus on the comparison of the low resolution and high resolution IFS-COMPO runs using global emissions. The runs compared use the following resolutions:

- Low resolution : T_L511, the current operational resolution (~40 km grid cell)
- High resolution : $T_{CO}1279$, the current deterministic NWP resolution (~9km grid cell)

In this section, global budgets are shown as well as evaluation of simulated fields against observations.

Budgets:

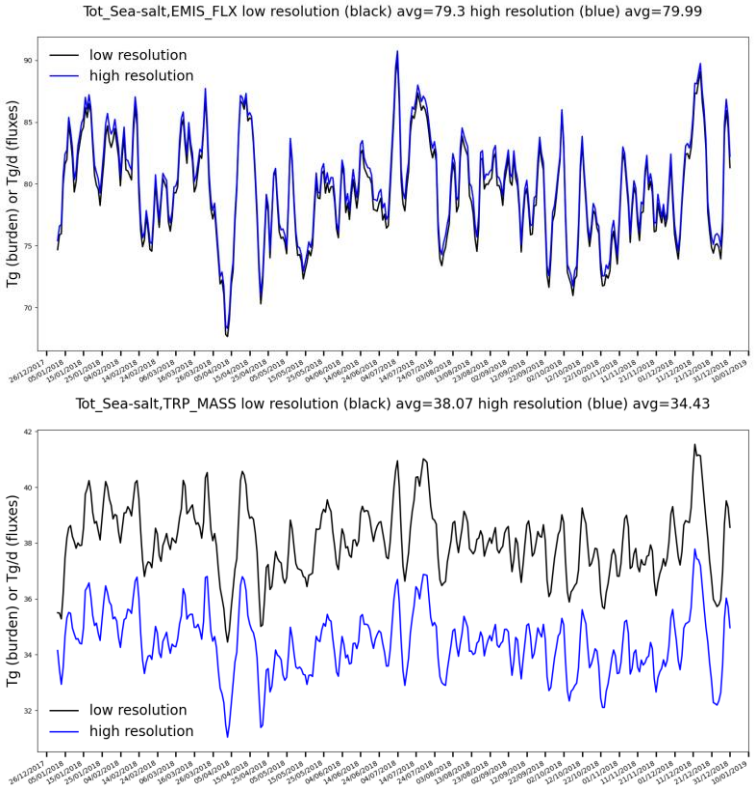

Figure 2.6: Global emissions and tropospheric burden of sea-salt aerosol (sum of the three bins)

For the sea-salt aerosols, we display the budgets for the total sea-salt aerosols (sum of the three bins) and we observe that the emissions are higher for the high resolution experiment, however the burden is lower than the low resolution case.

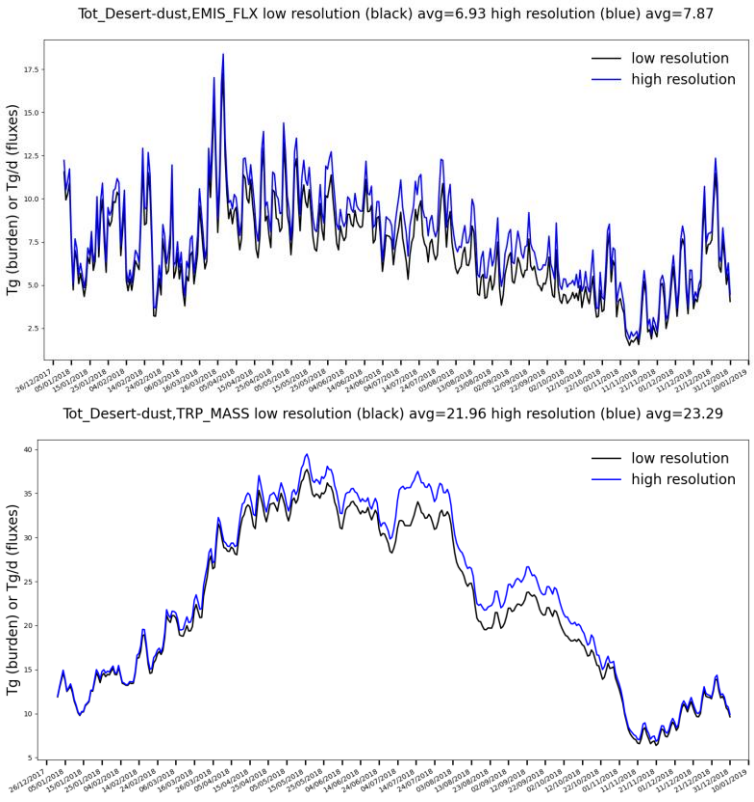

Figure 2.7: Global missions and tropospheric burden for desert dust

The budgets for the total desert dust show that the high resolution experiment has higher emissions and tropospheric burden.

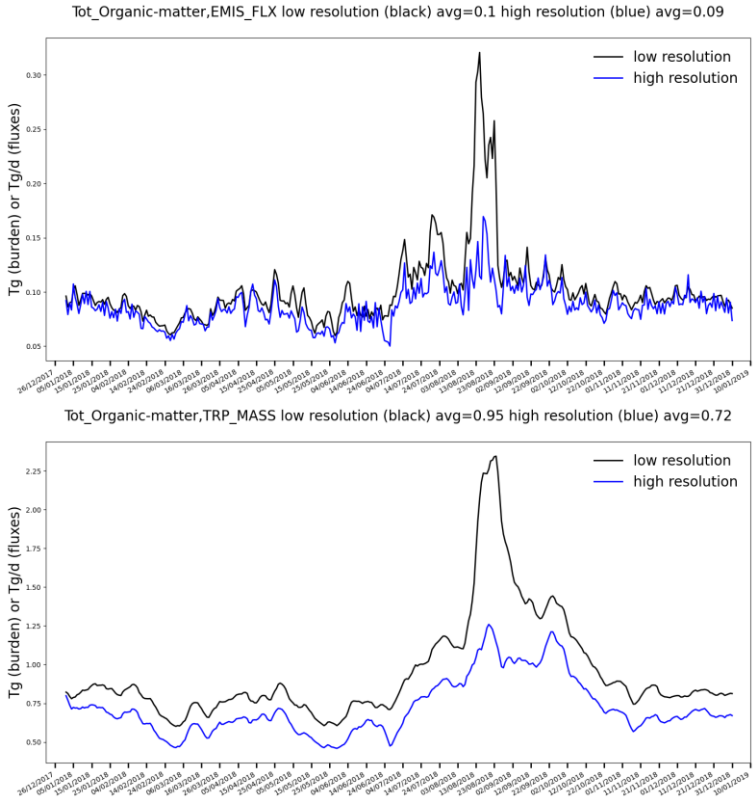

Figure 2.8 : Global emissions and tropospheric burden for organic matter

For the organic matter, the emissions are lower with high resolution, although emissions are not dynamically computed in IFS-COMPO, they are the sum of anthropogenic (CAMS_GLOB_ANT) and biomass burning (GFAS) emissions. The burden is significantly lower with high resolution.

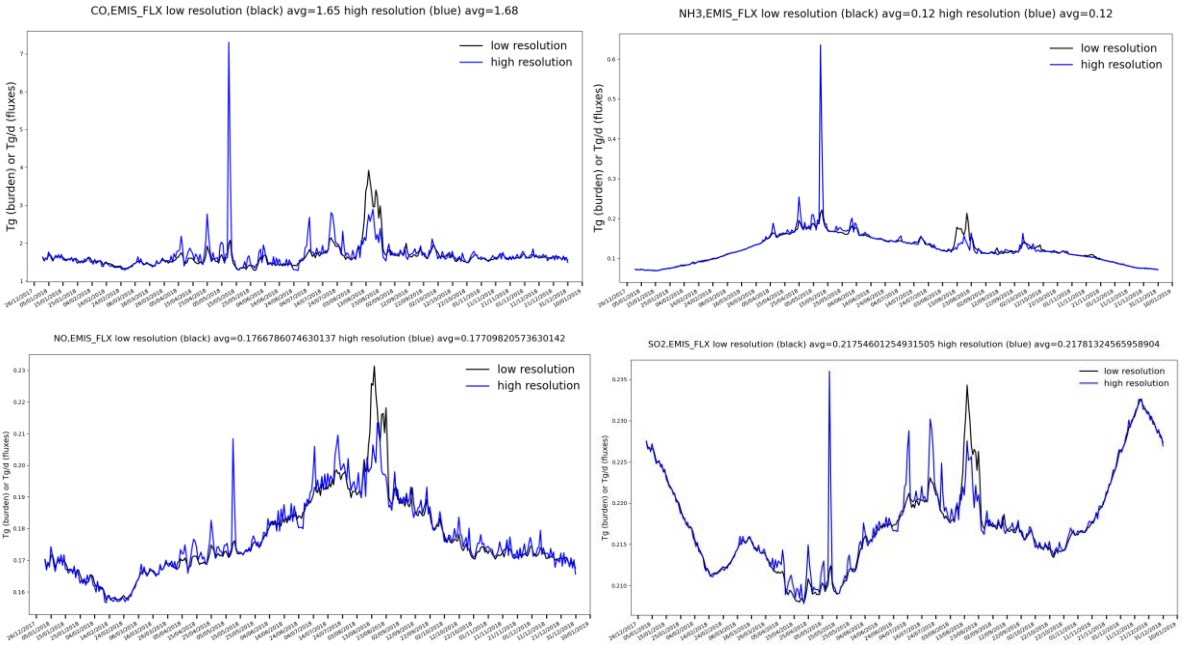

Figure 2.9 : Global emissions for different chemical species

Concerning the emissions, some extreme emissions occur at high resolution for all species. This could be caused by biomass-burning emission inputs although this needs to be confirmed.

In the following, we focus on the month of June 2018.

AOD and dust AOD

Figures 2.10 and 2.11 show simulated AOD at 550nm with the high resolution experiment and the relative difference to the low resolution experiment averaged in June 2018

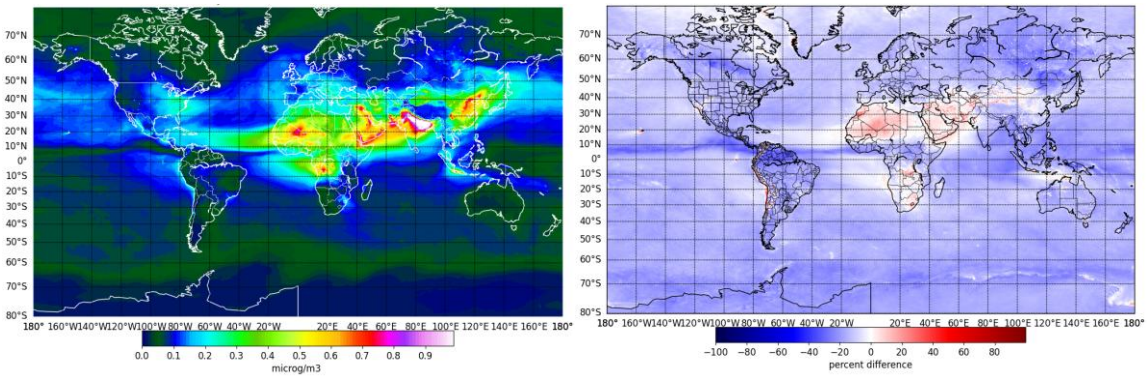

Figure 2.10 : Average simulated AOD at 550 nm at high resolution and relative difference for June 2018

High resolution is 15 to 25% lower in general except over dusty regions. ITCZ is clearly visible, maybe enhanced wet deposition?

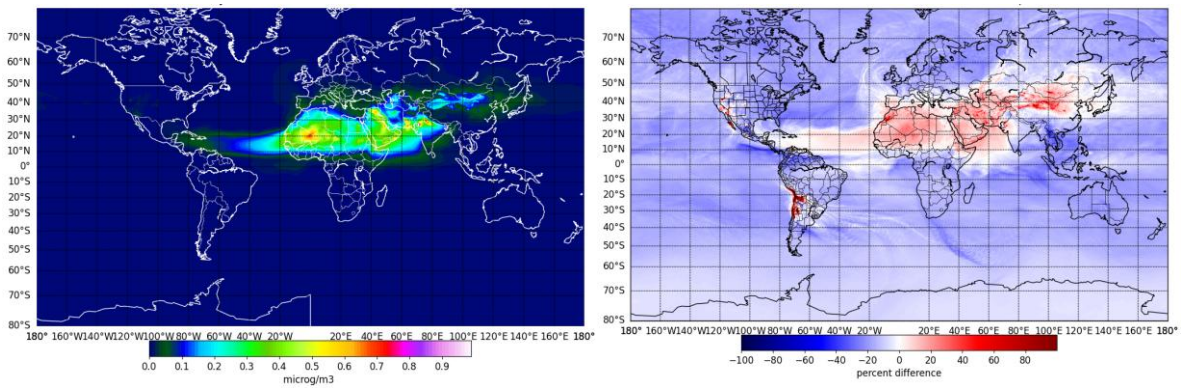

Figure 2.11 : Average simulated Dust AOD at 550 nm at high resolution and relative difference for June 2018

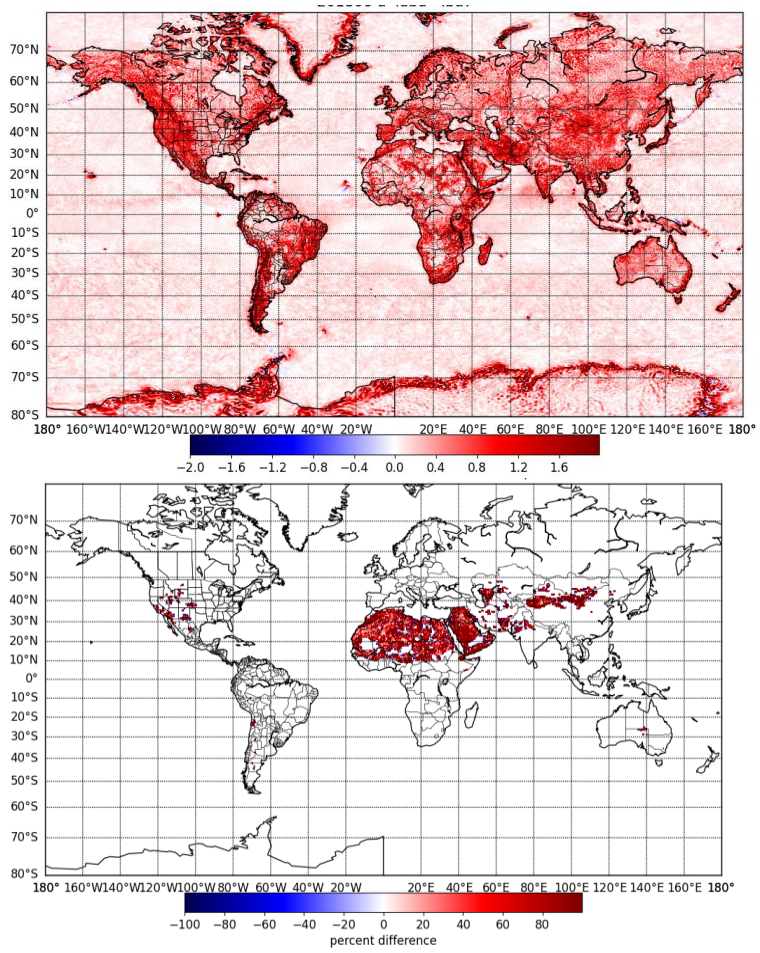

Figure 2.12 : Top, absolute difference of wind speed for June 2018 (high resolution - low resolution). Bottom, relative difference in the simulated desert dust emissions (high resolution % low resolution).

For the dust AOD, the high resolution case is 10 to 20% higher over source and outflow regions, and is lower elsewhere. Orography brings a larger increase. We also observe the wind speed is higher at high resolution, which means higher emissions and dry deposition of dust, which explains the higher AOD over the main emitting and outflow regions, and the lower values (from enhanced dry deposition) over regions far away from deserts. The increase of the emissions is particularly significant over mountain areas. The inputs of the dust emission scheme (dust source function) are at 0.5° resolution in the two configurations.

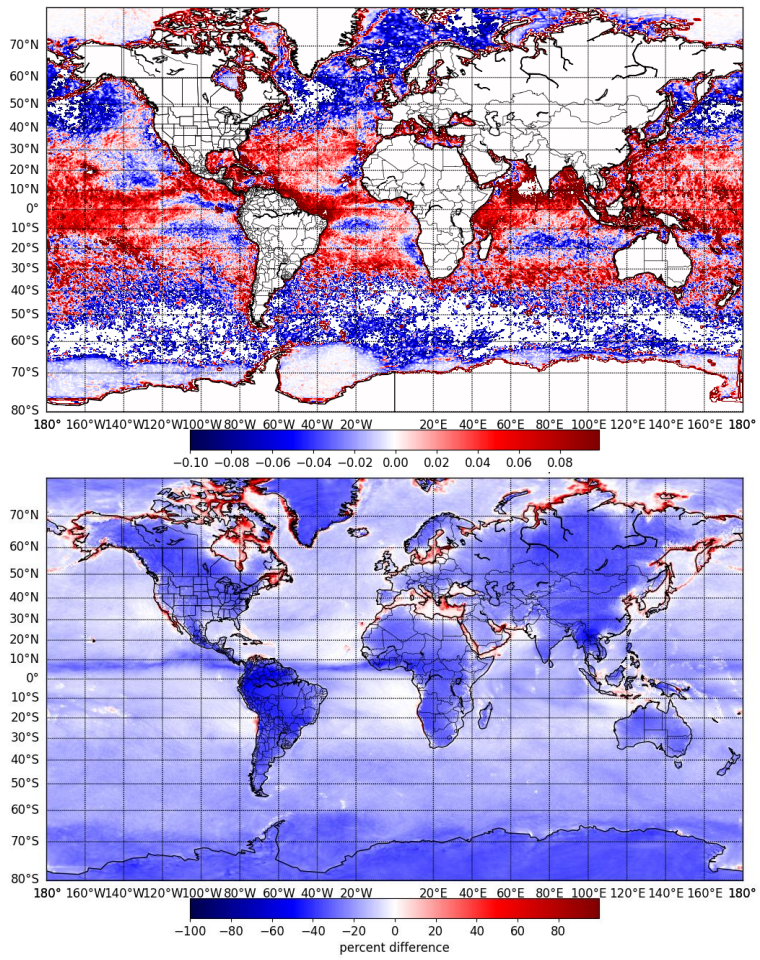

Figure 2.13 : Top, absolute difference of sea-salt emissions and bottom, relative difference of sea-salt AOD at 550 nm for June 2018

As for dust, the increase in simulated wind speed at high resolution leads to higher emissions of sea-salt aerosols particularly over equatorial and tropical regions. The sea surface temperature (SST) possibly plays a role to explain the lower emissions in extra tropical regions. The burden is lower at high resolution because of increased dry deposition, relatively more significant for smaller bins, which contribute relatively more than the super coarse bin to sea-salt AOD.

PM2.5

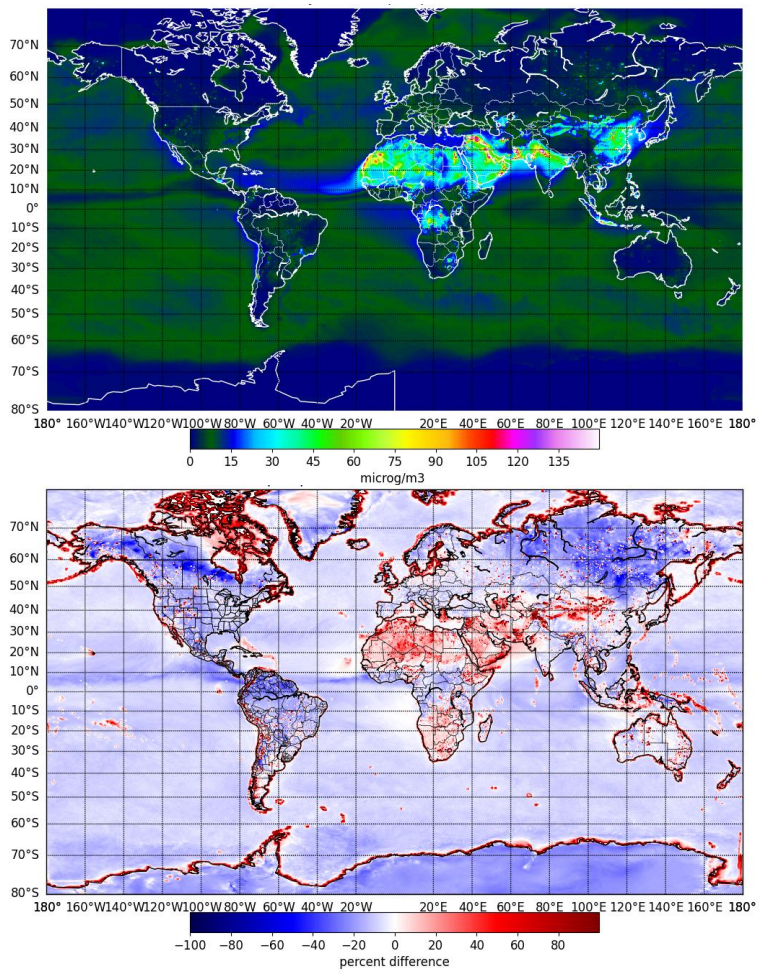

Figure 2.14 : Top, average simulated PM2.5 at high resolution and bottom, relative difference for June 2018

In general, the high resolution result is 10 to 20% lower for PM2.5, except over the dusty regions, the coastal areas and the islands, where the differences are larger. The coastline precision underlines the importance of a smooth or rough terrain for dry deposition and PM2.5 simulation.

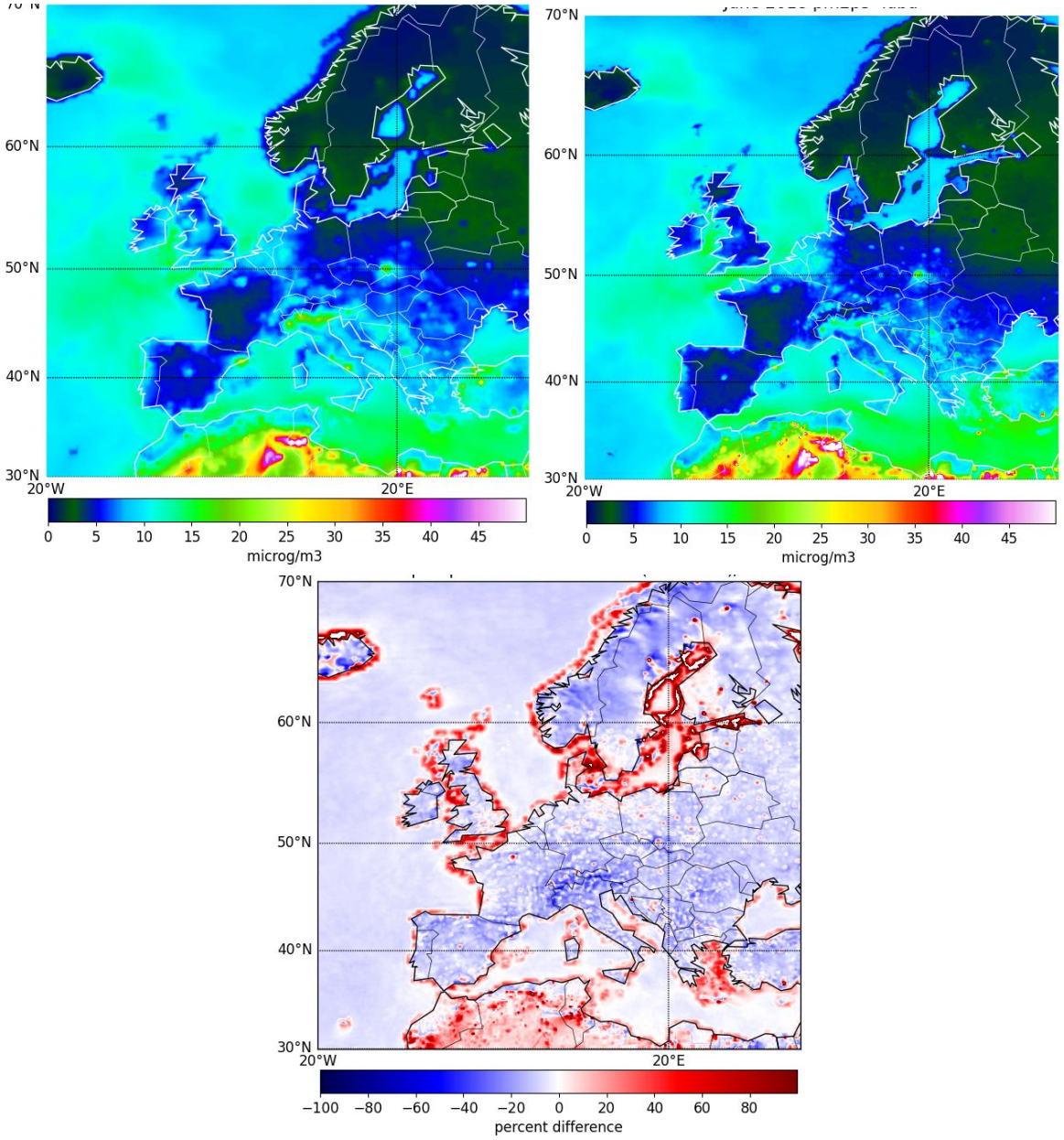

Figure 2.15: Top, average simulated PM2.5 at low (left) and high (right) resolution, and bottom, relative difference for June 2018.

If we focus on Europe, we observe higher values using high resolution over cities and genrally lower values in the rural countryside. backgrounds. The differences due to the orography and coastlines are clearly significant. This is also the case for PM10 simulations.

Evaluations of simulated PM2.5

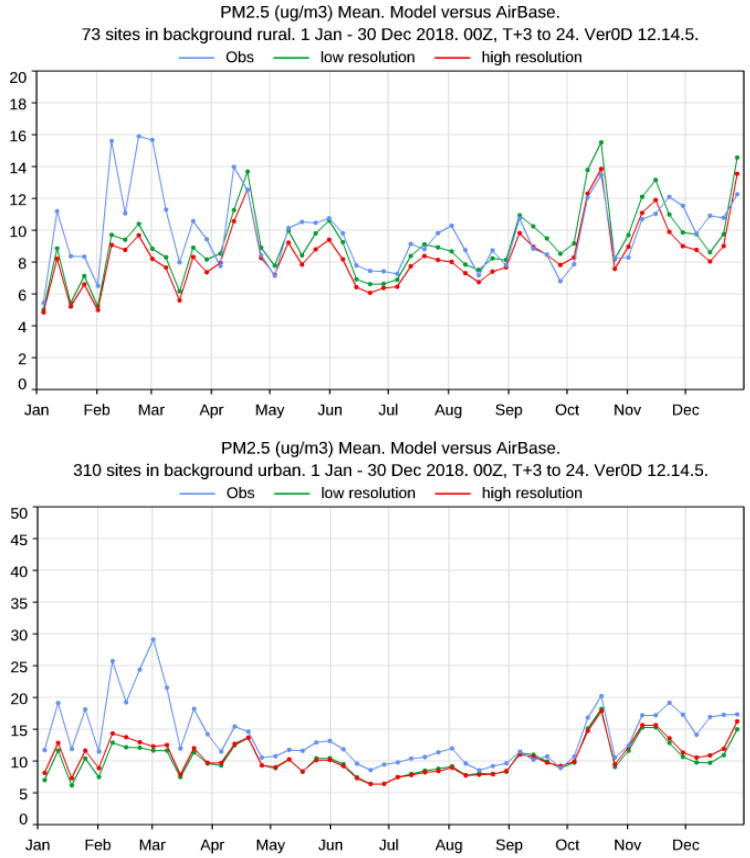

Figure 2.16 : Evaluations of daily PM2.5 at low and high resolution, for Europe, rural (top) and urban (bottom) background EEA/Airbase stations.

For Europe, the impact of the resolution is on simulated PM2.5 is relatively small. Over background rural stations, the simulated values are consistently lower with the high resolution experiment, worsening a low bias, while over background urban stations, values are higher in wintertime with the high resolution experiment, which improves slightly a persistent and large low bias. The improvement of the urban stations clearly come from a better representation of urban sources associated with the increased horizontal resolution. We see a similar feature over China (Figure 2.17), where the increased resolution brings an increase of simulated PM2.5 in wintertime over the North China Plain, dominated by urban centers.

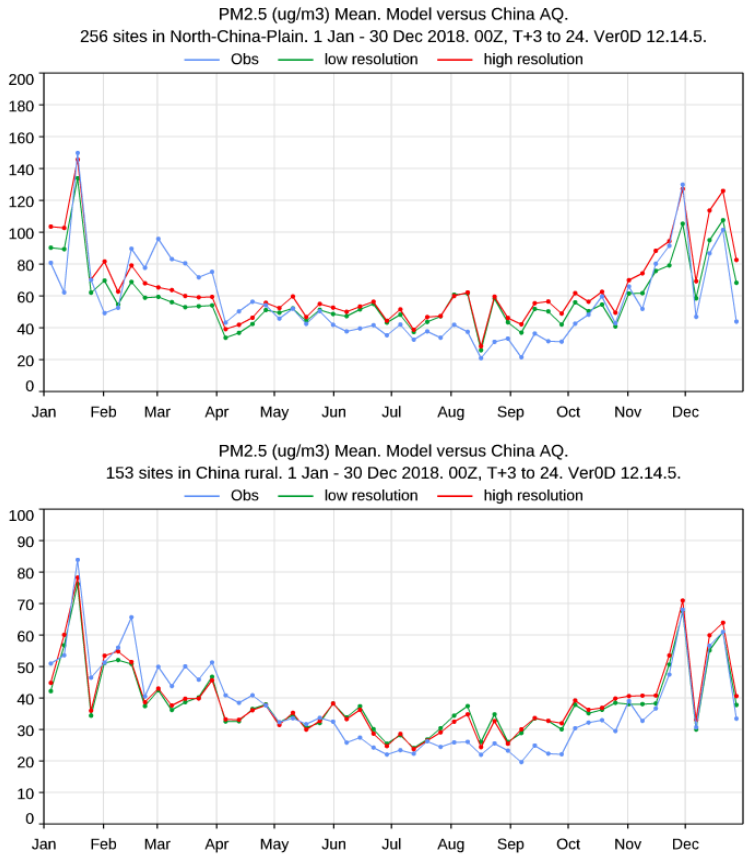

Figure 2.17 : Evaluations of daily PM2.5 at low and high resolution, for North China Plain and China rural background

In figure 2.18, we focus on the simulated diurnal cycle of PM2.5 over a heavily urban area (North China Plain). The diurnal cycle is clearly more intense with the higher resolution experiment as compared to lower resolution, and both show a much stronger diurnal cycle than what the observations indicate. This could be caused by a lower simulated boundary layer with the higher resolution experiment over urban centers (see Figure 2.19 and 2.20).

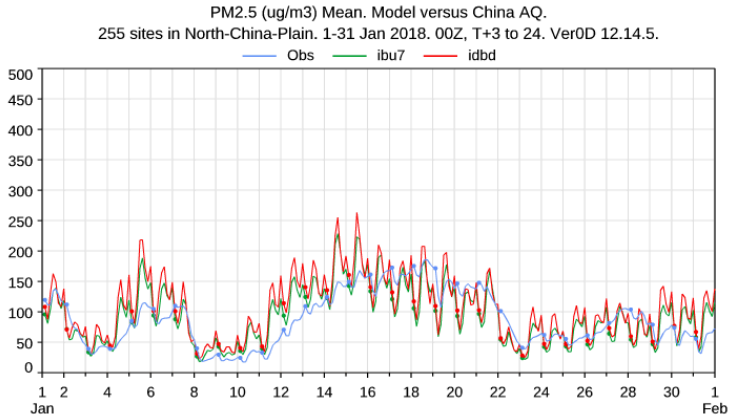

Figure 2.18 : Evaluations of three-hourly PM2.5 at low and high resolution, for North China Plain in January 2018

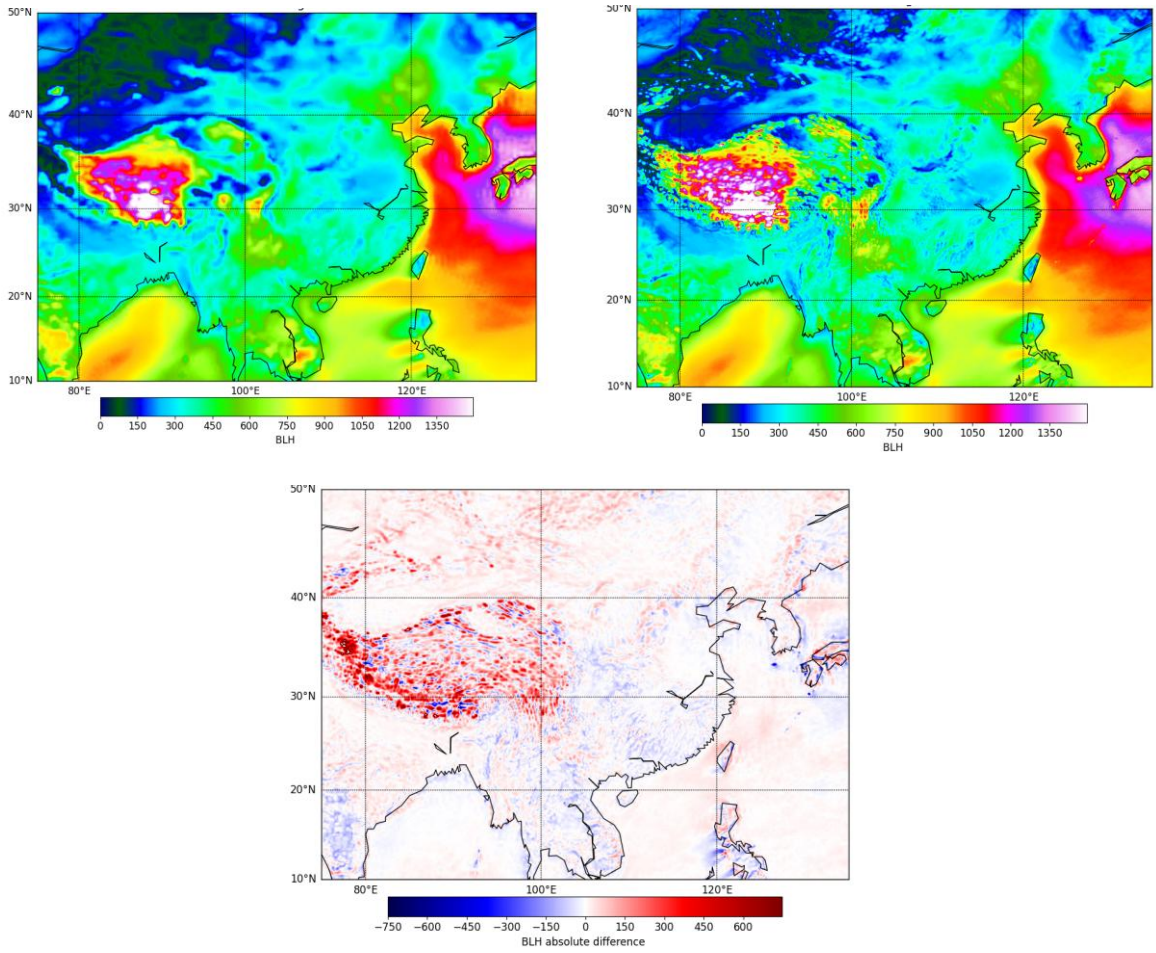

Figure 2.19 : Top, average boundary layer height in meters over China for January 2018 at low (left) and high (right) resolution, and absolute difference (bottom).

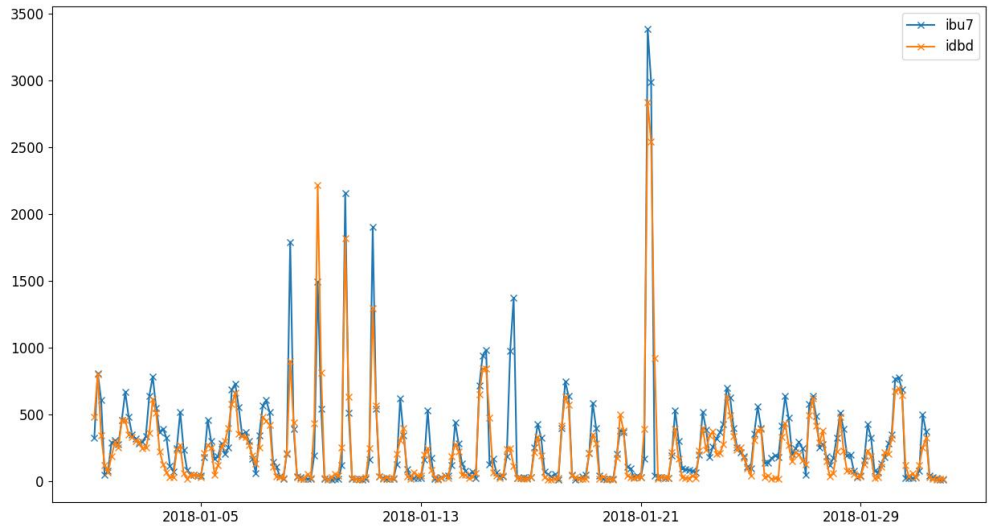

Figure 2.20 : Simulated 3 hourly boundary layer height (in meters) at Beijing in January 2018. Low resolution (blue) and high resolution (orange).

Figures 2.21, 2.22 and 2.23 show the impact of the resolution on simulated trace gases at surface : NO_2 and O_3 and CO over background rural stations in China, North America and Europe. For NO_2, the impact of resolution is significant, with higher values simulated at surface over China and lower over North America and Europe. These different results could be because of the higher density of large urban centers (better represented with high resolution experiments) over China than over N. America and Europe. For surface Ozone, significant differences in terms of evaluation occur mainly over Europe, with a much higher simulated values, matching the lower simulated NO_2 values with high resolution. Finally, for CO, the simulated values are often lower with the high resolution experiment.

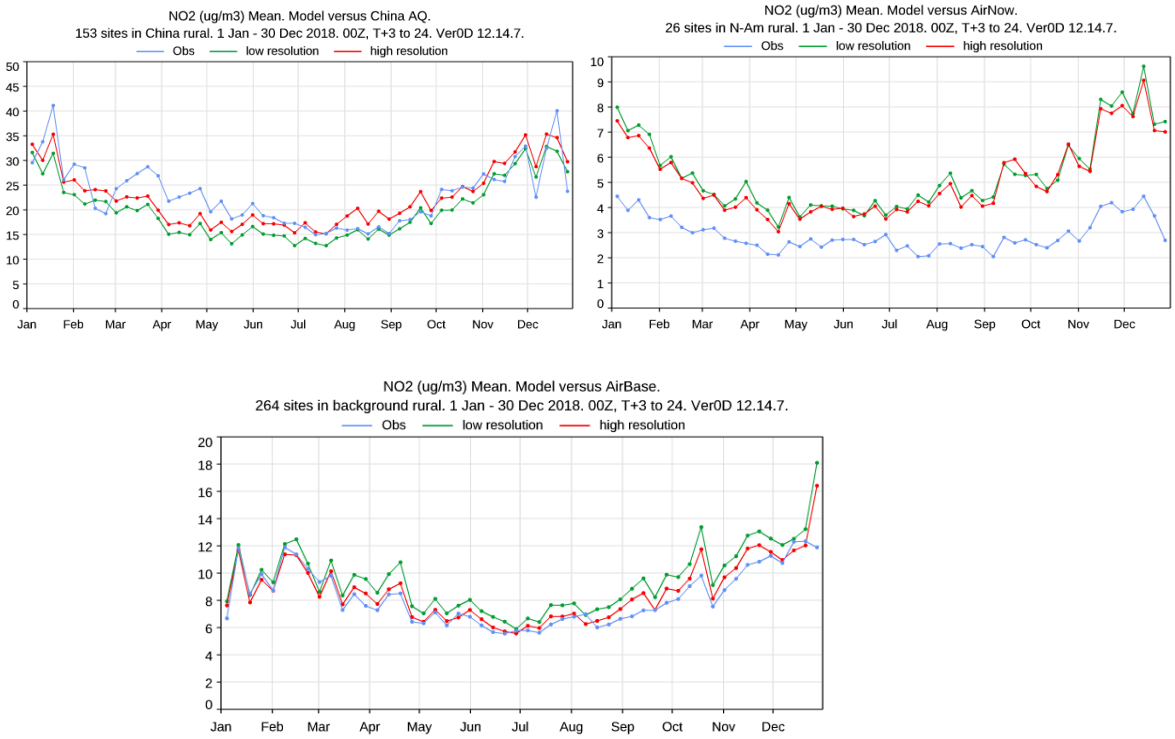

Figure 2.21 : Evaluations of NO_2 at low and high resolution, for China rural background (top right), North America rural background (top left), and European rural background (bottom) stations.

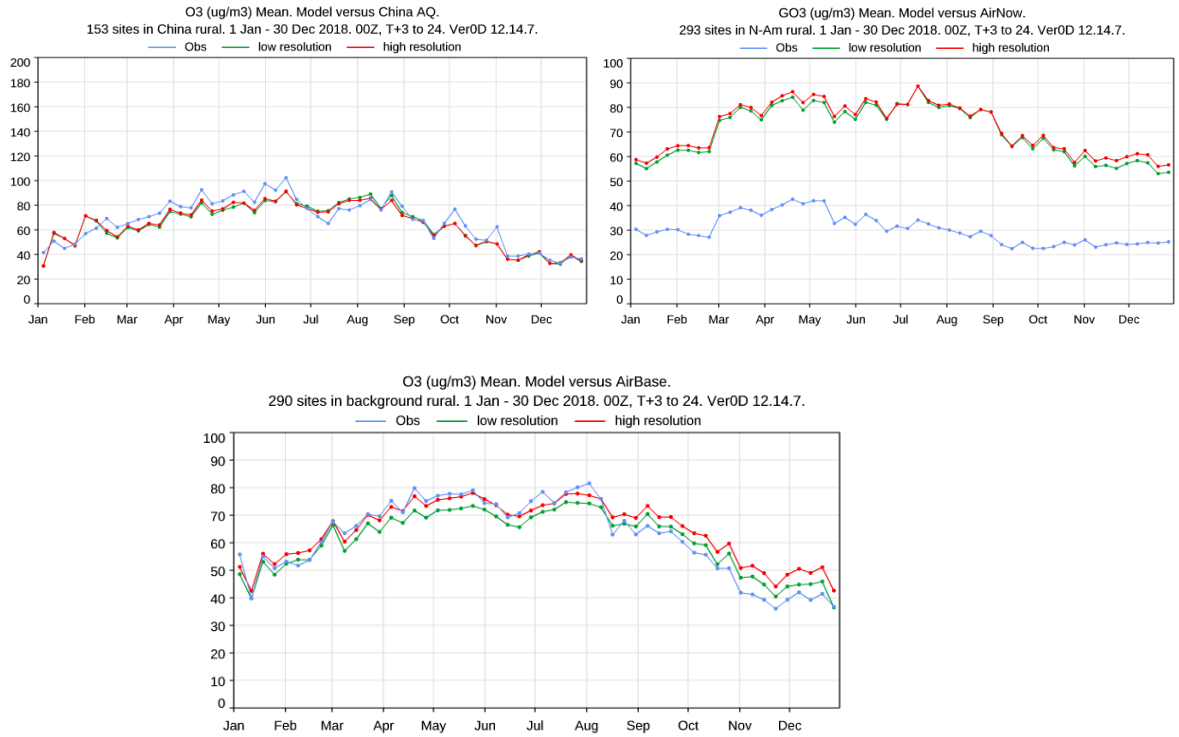

Figure 2.22: Evaluations of O_3 at low and high resolution, for China rural background (top right), North America rural background (top left), and European rural background (bottom) stations.

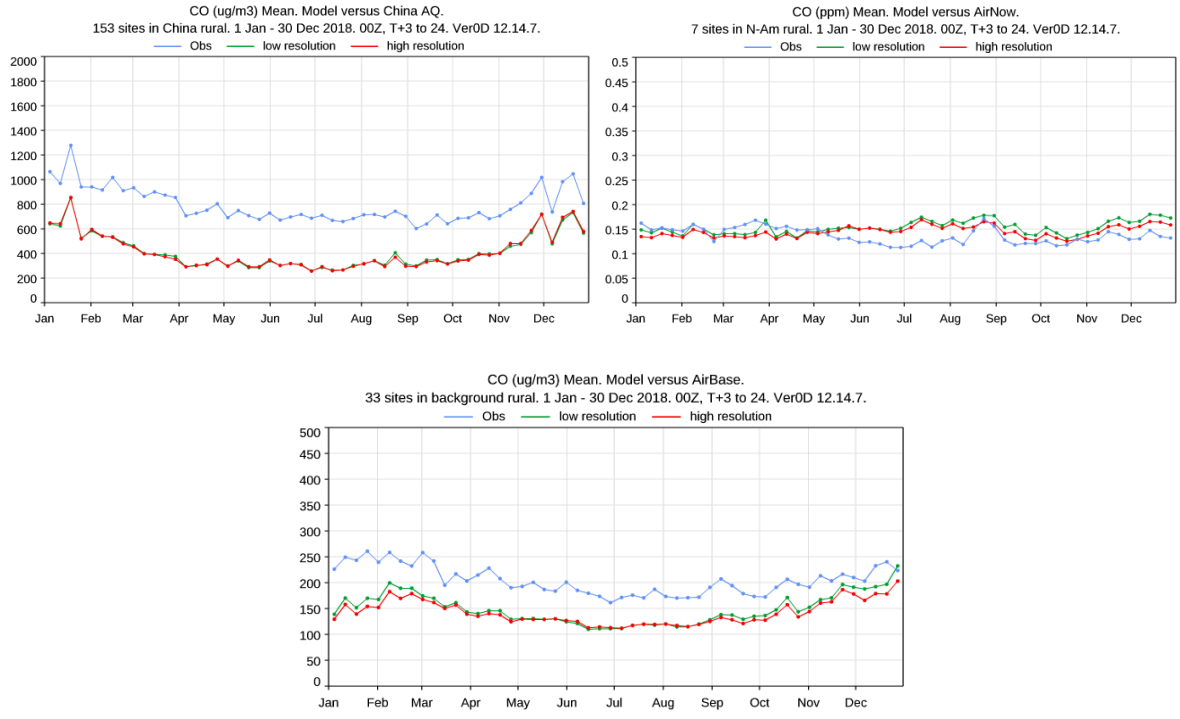

Figure 2.23 : Evaluations of CO at low and high resolution, for China rural background (top right), North America rural background (top left), and European rural background (bottom) stations.

4.4 Conclusion for the IFS-COMPO preparation for intercomparison

The global CAMS system has been run with a recent cycle using emissions (over Europe) and a resolution used by the CAMS regional systems, in order to be compared against similar simulations by the regional models, presented in section 4. This allowed a better understanding of the impact of the differences in the emissions used, as well as a first study of using IFS-COMPO at a very high resolution. The change in resolution impacted meteorological fields (temperature, precipitation, thermal stratification), with significant impacts on the online emissions of desert dust and sea-salt, as well as on the dry and wet deposition of all species.

Intercomparison and evaluation of regional and global models

5.1 Analysis framework

The objective of this analysis was to evaluate and compare the outputs of global and regional atmospheric composition models, with a particular focus on the year 2018. The intercomparison targeted particulate matter, specifically PM10 and PM2.5. To ensure consistency across model evaluations, all analyses were conducted on a common spatial framework corresponding to the CAMS regional domain with a horizontal resolution of 0.1° × 0.1°.

Regional models were driven by meteorological inputs from the Integrated Forecasting System (IFS-COMPO), with data provided at a temporal resolution of three hours. Similarly, chemical boundary conditions (BCs) were supplied by the IFS-COMPO global system at the same temporal resolution, ensuring coherent and dynamically consistent lateral input across regional simulations.

A multifaceted methodological approach was employed to interrogate the model outputs. These included:

- **Spatial maps of concentrations** and **difference maps** to visually assess the geographical distribution of modelled pollutants and identify spatial discrepancies between models.
- **Histograms** to characterize the frequency distribution of pollutant concentrations across the domain, highlighting tendencies such as over- or underestimation by individual models.
- **Time series analyses**, presented at both daily and monthly scales, are used to evaluate temporal trends in pollutant concentrations and associated error metrics.
- **Error matrices** that provided statistical summaries of model performance in terms of bias, root mean square error (RMSE), and other standard indicators.
- **Quantile-Quantile (Q-Q) plots**, used to compare the statistical distributions of modelled and reference data, thereby enabling the identification of systematic deviations across concentration ranges.

To capture the diversity of atmospheric and geographical conditions across Europe, the model intercomparison study encompassed seven distinct regions. These regions were selected based on their contrasting climatological, topographical, and emission characteristics that are critical factors influencing the formation and dispersion of particulate matter. The inclusion of a broad geographic spread enhances the robustness of the evaluation and supports a better understanding of model performance under varying environmental contexts.

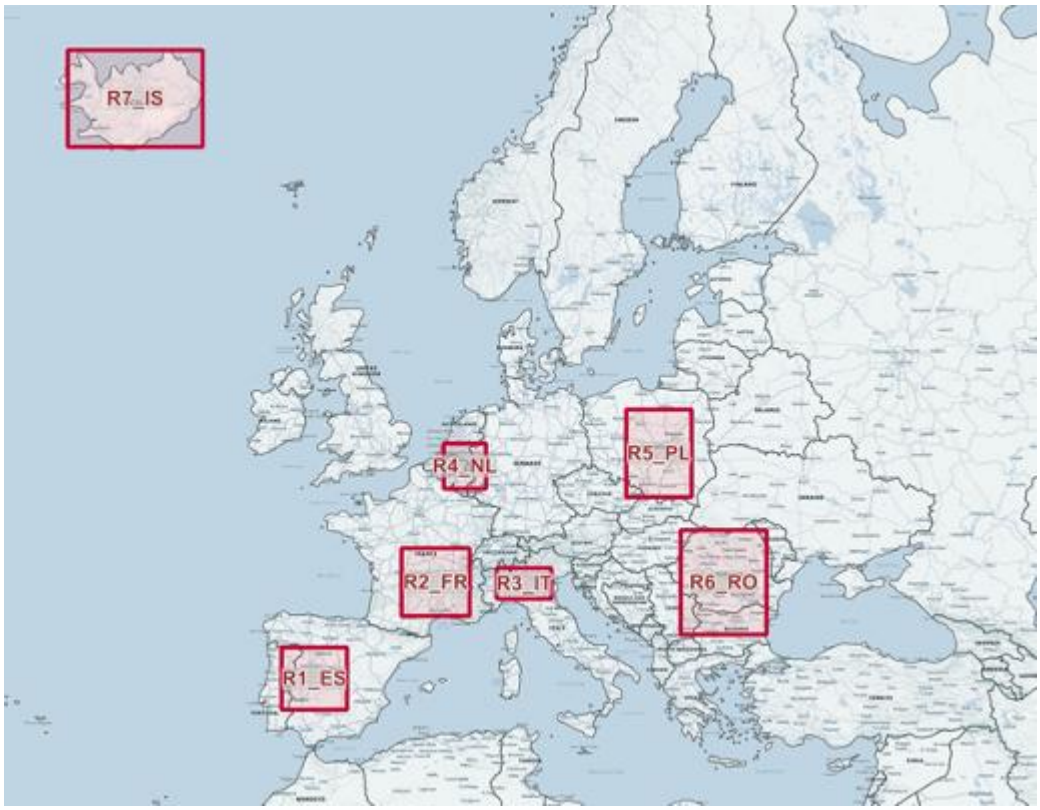

Figure 3.1 Location and spatial extend of analysed regions for intercomparison and evaluation over Europe

For each region, ground-based observational data of PM10 and PM2.5 concentrations were used to evaluate model outputs (source: EEA). The number of stations varied by region and pollutant, reflecting differences in network density and monitoring priorities.

The regions and associated observational coverage are summarized as follows (Table 1):

Table 3.1. PM10 and PM2.5 air quality monitoring stations were used for the evaluation

Region code	Country/region	PM10 number of stations	PM2.5 number of stations
R1_ES	Spain	38	12
R2_FR	France	62	25
R3_IT	Italy	59	36

R4_NL	The Netherlands	69	49
R5_PL	Poland	136	67
R6_RO	Romania	55	22
R7_IS	Iceland	5	4

The variation in the number of stations across regions influenced the statistical significance of the evaluation. For instance, regions such as Poland and the Netherlands, with extensive monitoring networks, provided higher spatial representativity and allowed for more reliable validation analyses. In regions with sparser station coverage, such as Iceland, the evaluation results are more localized and subject to higher uncertainty. Nevertheless, the inclusion of such regions remains valuable, as they offer insights into model performance under unique environmental conditions, such as low population density and the impact of boundary conditions.

5.2 IFS-COMPO sensitivity analysis over Europe

5.2.1 Sensitivity of IFS-COMPO results to emission datasets

This section examines the sensitivity of the IFS-COMPO model to changes in emission data over Europe, comparing results from the CAMS regional inventory (further referred to as REG) and the CAMS global inventory (further referred to as GLOB)

5.2.1.1 Spatial pattern by season

Across Europe, simulations driven by regional emission inventories consistently produced higher concentrations in known anthropogenic hotspots, particularly during the winter months (DJF, SON). These regions include densely populated urban areas and major industrial zones, where emission intensities are greatest and atmospheric dispersion is typically limited due to stable meteorological conditions. In contrast, lower concentrations were observed over water bodies, such as the North Sea and the Mediterranean, reflecting both reduced local emissions and enhanced mixing. This land–sea contrast was most pronounced during spring (MAM) and summer (JJA), with regional emissions yielding lower concentrations over the North Sea in spring and over the eastern Mediterranean in summer.

The annual mean PM_{10} concentration differences between simulations using regional and global emissions were found to be strongly biased by differences during the cold season.

CAMAERA

Comparative results between simulations conducted at two spatial resolutions (0.5° and 0.1°) showed that the spatial patterns of concentration differences were remarkably consistent across resolutions. This suggests that the impact of emission inventory choice dominates over the resolution effect in shaping large-scale patterns, although fine-resolution simulations remain important for resolving localized features.

In general, simulations using regional emissions led to higher concentrations across most of Europe, especially over urban and industrialized areas. However, exceptions were observed in Switzerland and Turkey. These discrepancies may reflect differences in the spatial allocation or magnitude of sector-specific emissions in the global inventories.

Northern Europe, Northern Africa, and open ocean areas showed minimal or no differences between the two emission data sets. This indicates that natural emissions (e.g., sea salt, dust) do not significantly contribute to the observed differences, highlighting that the variability is predominantly attributable to anthropogenic source inputs.

	0.5x0.5 deg	0.1x0.1 deg
Year	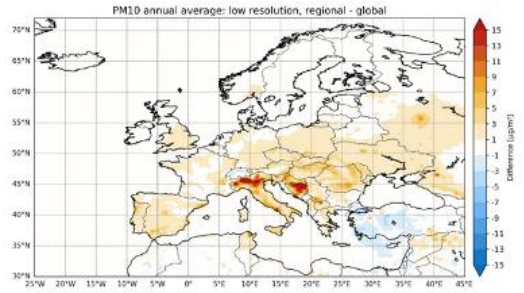	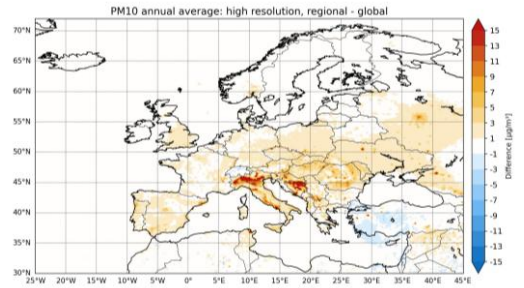
DJF	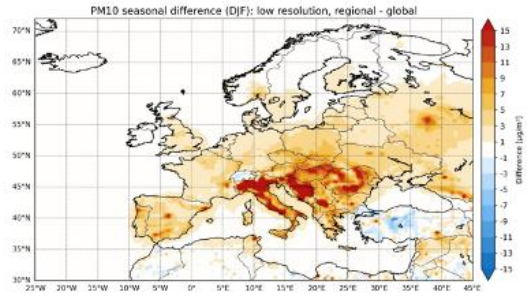	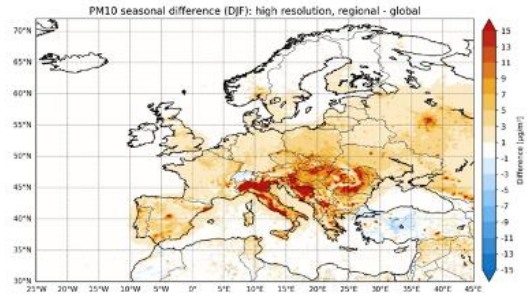
MAM	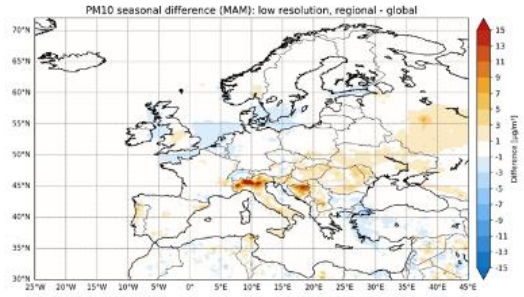	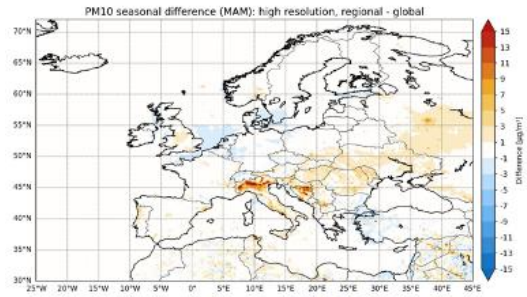

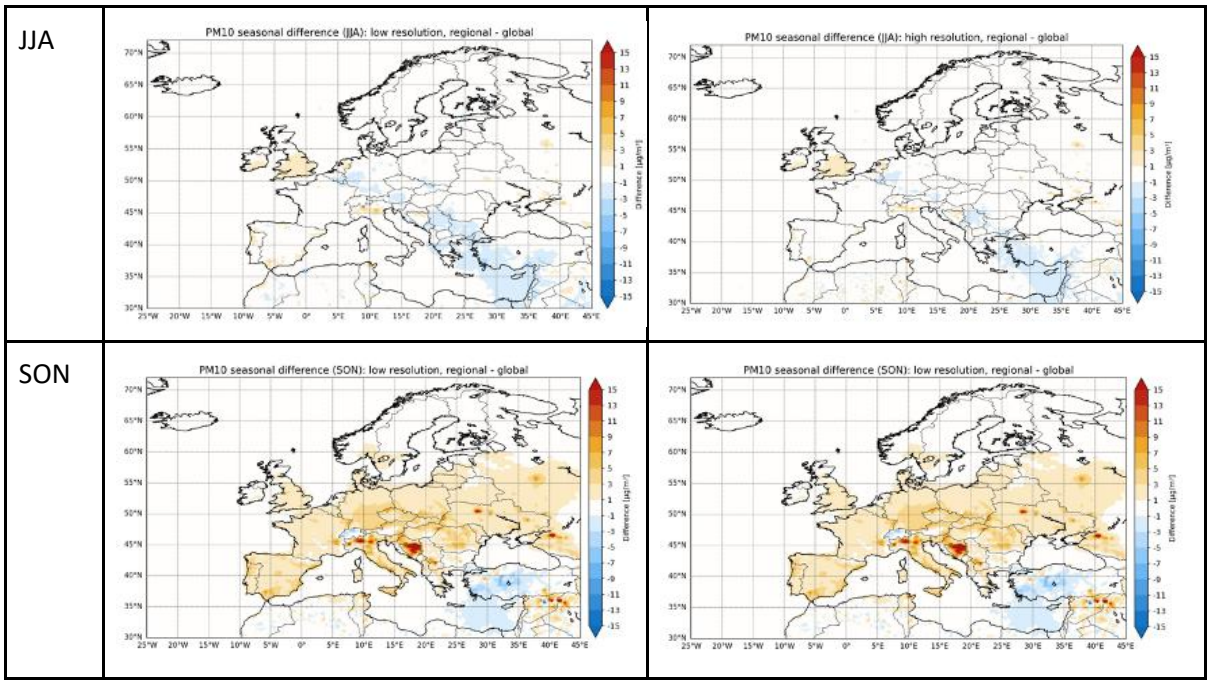

Figure 3.2. PM10 concentration delta between results obtained with the REG emission inventory and GLOB emission inventory calculated at 0.5deg (left panel) and 0.1 deg (right panel)

The emission sensitivity analysis for PM2.5 reveals a spatial and seasonal pattern that closely aligns with that observed for PM10. As with PM10, higher concentrations were consistently observed in simulations using regional emissions across much of continental Europe, particularly in urban and industrial hotspots. These differences were most pronounced during the winter months (DJF), reflecting the dominant influence of residential combustion.

The difference fields in DJF show increased magnitude and spatial coverage of concentration differences for PM2.5 compared to PM10, especially over densely populated regions. This may indicate not only higher wintertime emissions in the regional inventory but also potentially different temporal profiles, which may better represent seasonal variability — particularly for residential heating emissions that peak during colder periods. The stronger sensitivity in PM2.5 is also linked to its longer atmospheric residence time and its formation through secondary processes, which are highly dependent on both emissions and atmospheric chemistry.

Regions where higher concentrations were associated with global emissions remained largely consistent between PM10 and PM2.5. These include Turkiye and Switzerland, where global inventories yielded higher concentrations across all seasons. This could be due to differences in source representation, spatial allocation, or unresolved topographic influences in the global emission dataset. In spring (MAM), negative differences appeared over the North Sea and Baltic Sea, while in summer (JJA), they were observed over the eastern Mediterranean Sea and parts of Central Europe.

	0.5x0.5 deg	0.1x0.1 deg
Year	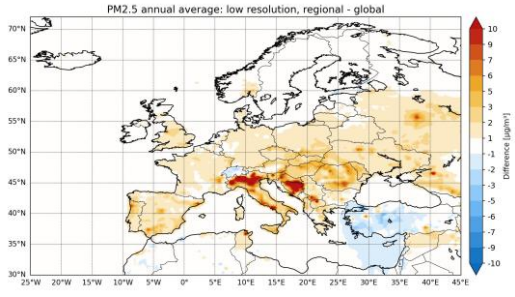	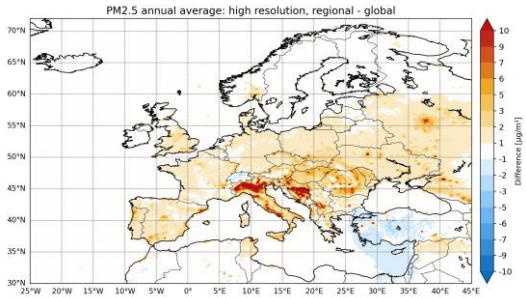
DJF	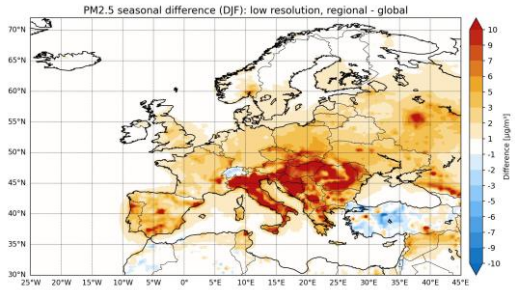	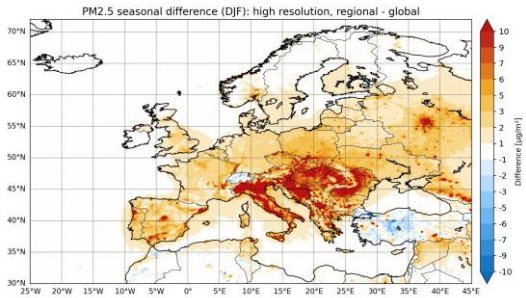
MAM	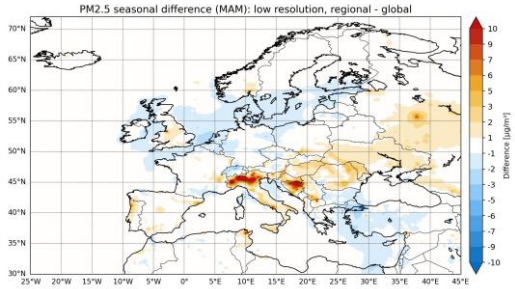	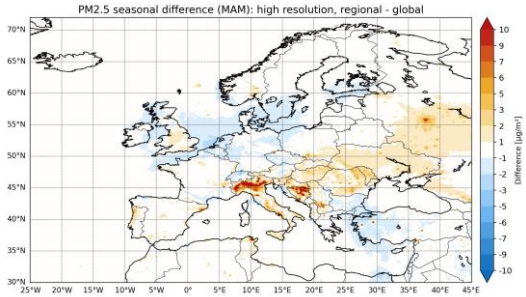
JJA	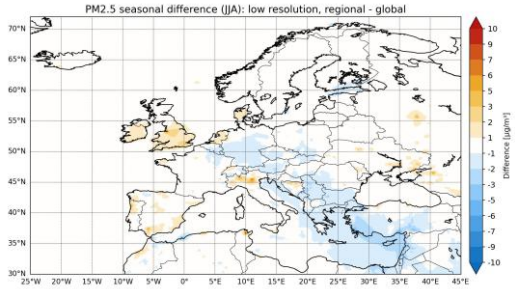	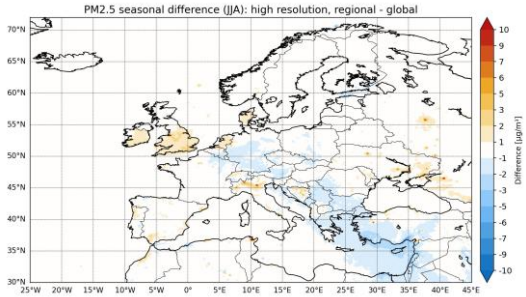

SON	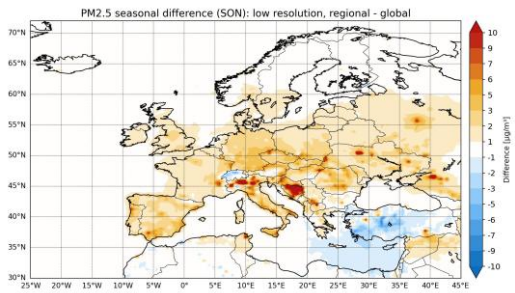	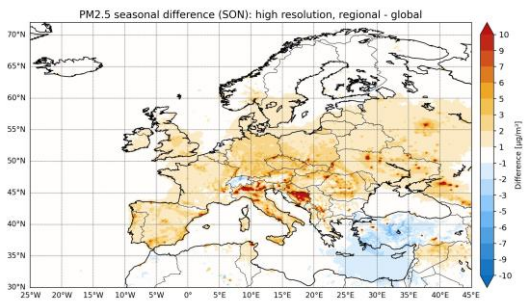

Figure 3.3. PM2.5 concentration delta between results obtained with REG emission inventory and GLOB emission inventory calculated at 0.5deg (left panel) and 0.1 deg (right panel)

5.2.1.2 Monthly time series by regions

The analysis of monthly averaged time series for individual regions supports and refines the patterns identified in the spatial analysis. In general, the temporal evolution of PM10 and PM2.5 concentrations reveals consistently similar seasonal behaviour across both spatial resolutions (0.5° and 0.1°), indicating that resolution effects have a limited impact on the overall temporal patterns when aggregated at the regional scale.

Simulations based on regional emissions consistently yield higher concentrations during the colder months, although the timing and magnitude of these differences vary by region. In Spain and France, elevated values in simulations using regional inventories are observed primarily in January, February, October, November, and December, with negligible differences during the warmer months (April through September). This reflects the strong seasonality of residential heating and its influence on air pollution levels during cooler periods.

In Poland and Romania, the period of elevated differences extends into March, indicating a longer heating season or a greater sensitivity of emissions to ambient temperature in these countries. Conversely, in the Netherlands, the variability is notably lower, with monthly mean differences between simulations generally constrained within a 10–15 µg/m³ range, and a flatter seasonal profile overall.

Iceland remains an exception throughout the analysis, with practically no difference observed between simulations using regional and global emissions. This is consistent with the limited anthropogenic source strength in the region, low population density, and the dominant role of long-range transport and natural sources.

	0.5x0.5	0.1x0.1
Spain	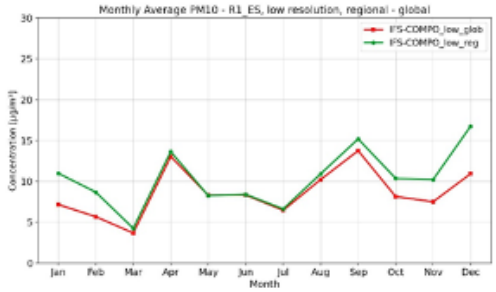	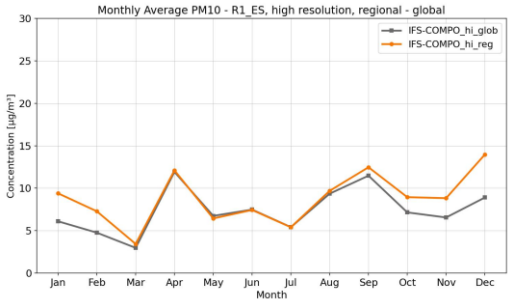
France	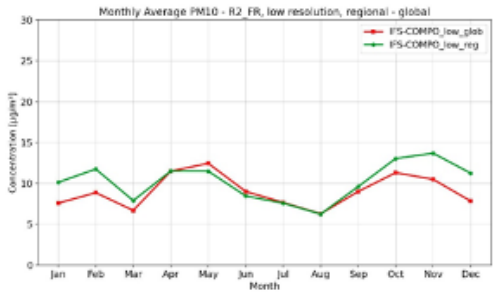	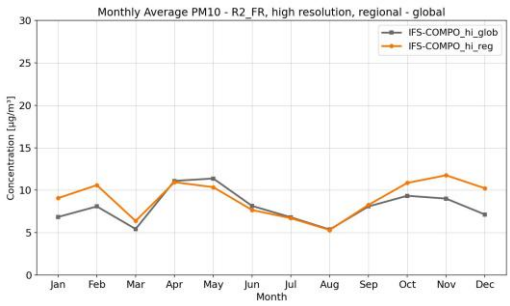
Italy	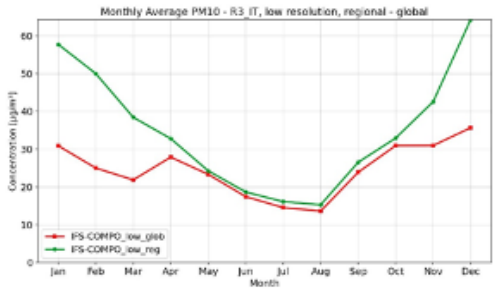	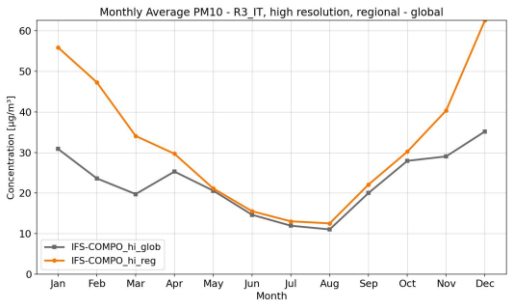
NL	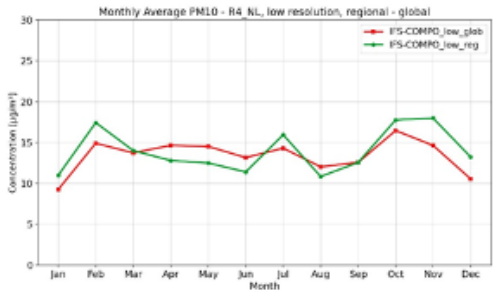	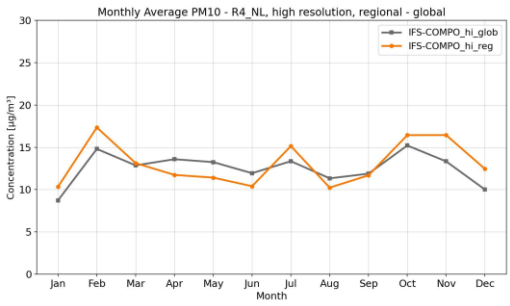
Poland	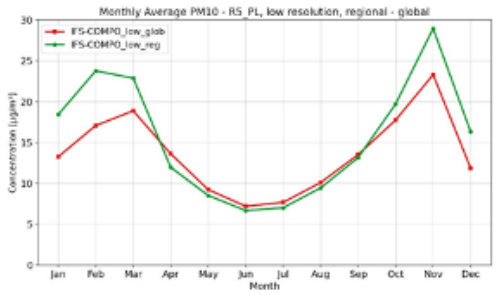	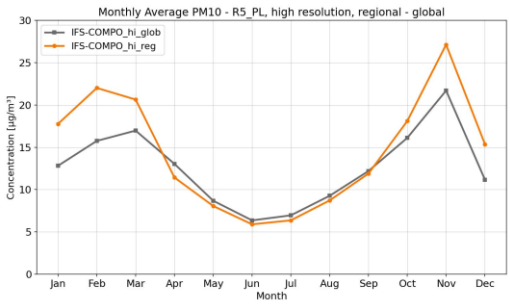

Romania	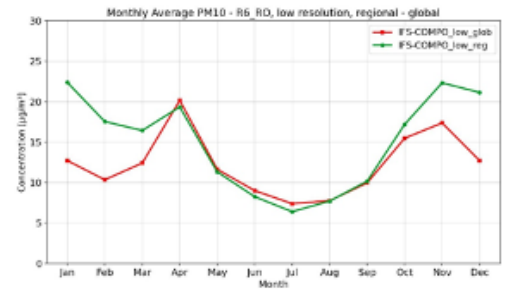	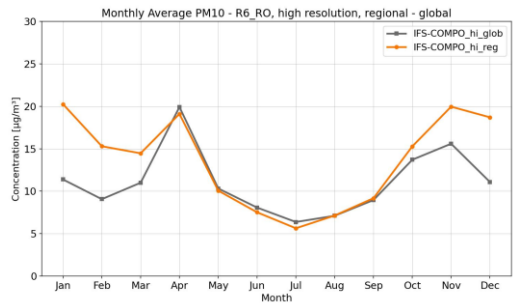
Iceland	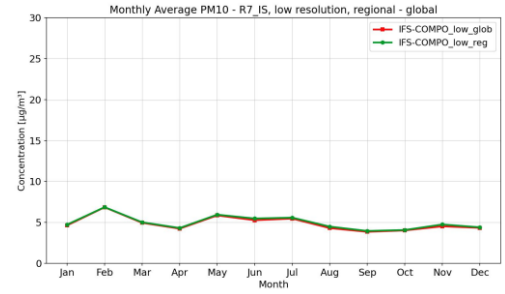	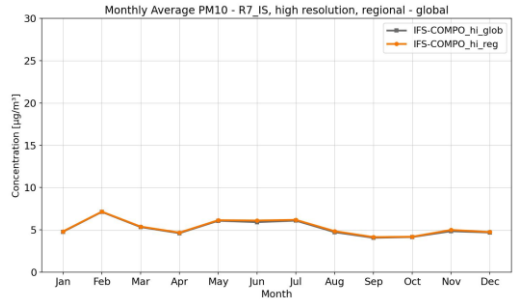

Figure 3.4. PM10 monthly concentrations obtained with the REG emission inventory and the GLOB emission inventory, averaged over individual regions, calculated at 0.5deg (left panel) and 0.1 deg (right panel)

	0.5x0.5	0.1x0.1
Spain	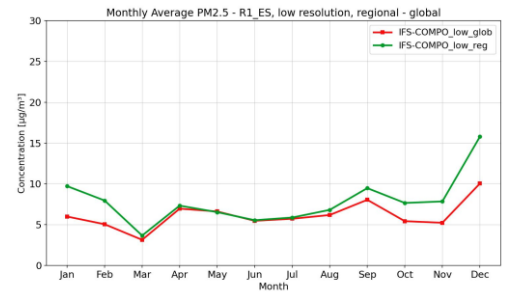	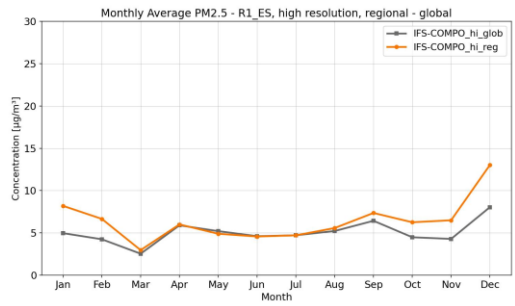
France	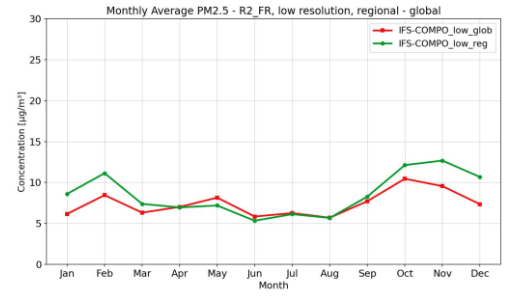	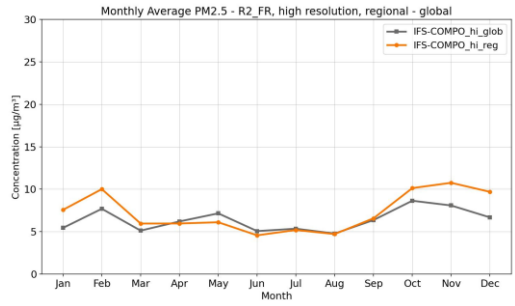

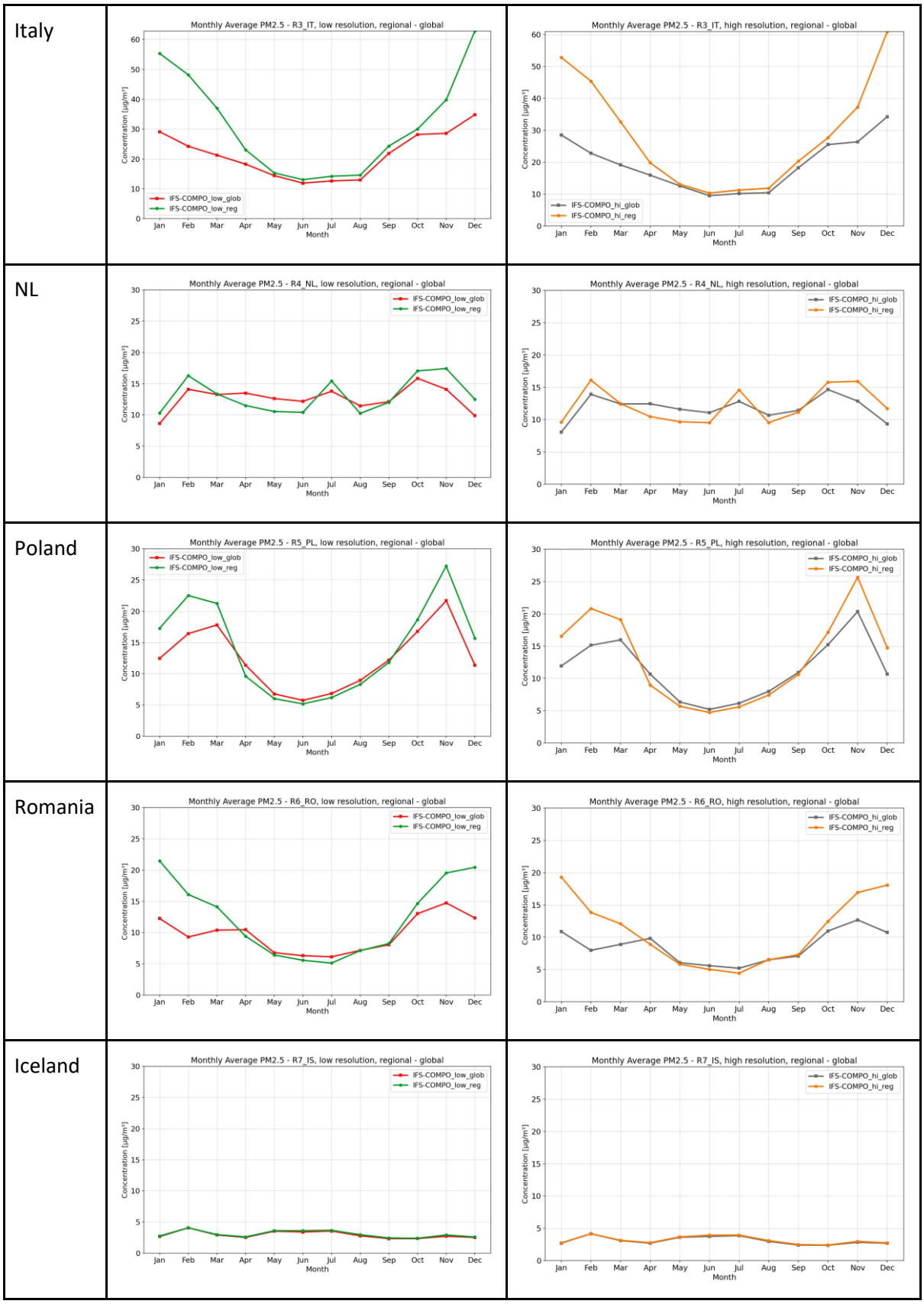

Figure 3.5. PM2.5 monthly concentrations obtained with the REG emission inventory and the GLOB emission inventory, averaged over individual regions, calculated at 0.5deg (left panel) and 0.1 deg (right panel)

5.2.2 Sensitivity of IFS-COMPO results to the computational grid resolution

This section investigates the sensitivity of the IFS-COMPO model to changes in the grid resolution, comparing results obtained with the grid resolution of ~0.5x0.5deg (further referred to as LOW) and the grid resolution~0.1x0.1 deg (further referred to as HIGH).

5.2.2.1 Spatial pattern by season

The PM10 concentration differences between simulations using different spatial resolutions—averaged annually and seasonally—are quite similar. For both emission datasets (global and regional), the main characteristics of the concentration fields remain consistent across resolutions.

The differences observed between higher (0.1 deg) and lower (0.5 deg) resolution simulations indicate that concentrations are generally higher over hotspots in the high-resolution setup, but tend to be lower in more remote areas. One possible explanation is related to the efficiency of dry deposition at higher resolution. This remains a hypothesis and would require further targeted investigation in collaboration with WP5. Additionally, concentrations at higher resolution are slightly elevated over water bodies along the coastlines, which may also be attributed to differences in dry deposition due to the differences in land-sea mask between resolutions.

Over ocean regions, concentrations calculated at the high resolution are lower. This is likely related to the representation of sea spray aerosol sources, which depend on surface wind speed. Differences in wind speed fields from the IFS meteorological forcing at different resolutions may result in different emission fluxes. In contrast, over North Africa, PM10 concentration differences (HIG - LOW) are positive, which could be associated with finer spatial representation of surface characteristics and possibly stronger surface winds, both of which can influence the uptake of desert dust.

PM10 concentration delta between the two resolutions is negligible across much of northern and eastern Europe. These regions are characterized by low emission intensities and relatively homogeneous meteorological and surface conditions. The limited impact of spatial resolution in such areas suggests that under low-emission regimes, the effect of resolution becomes less significant.

	GLOBAL	REGIONAL
Year	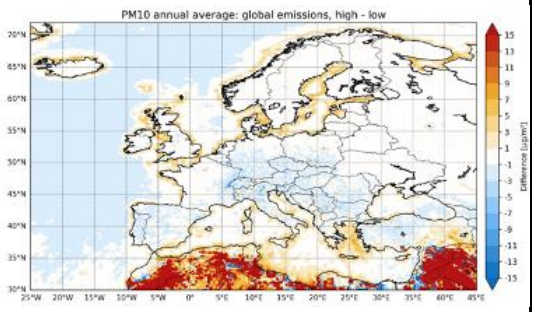	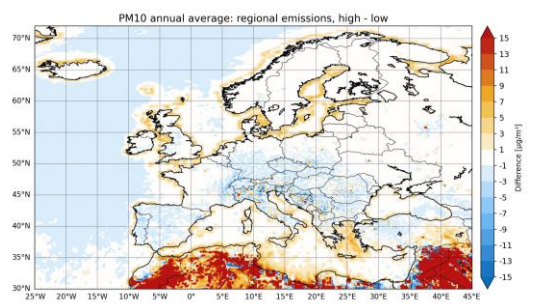

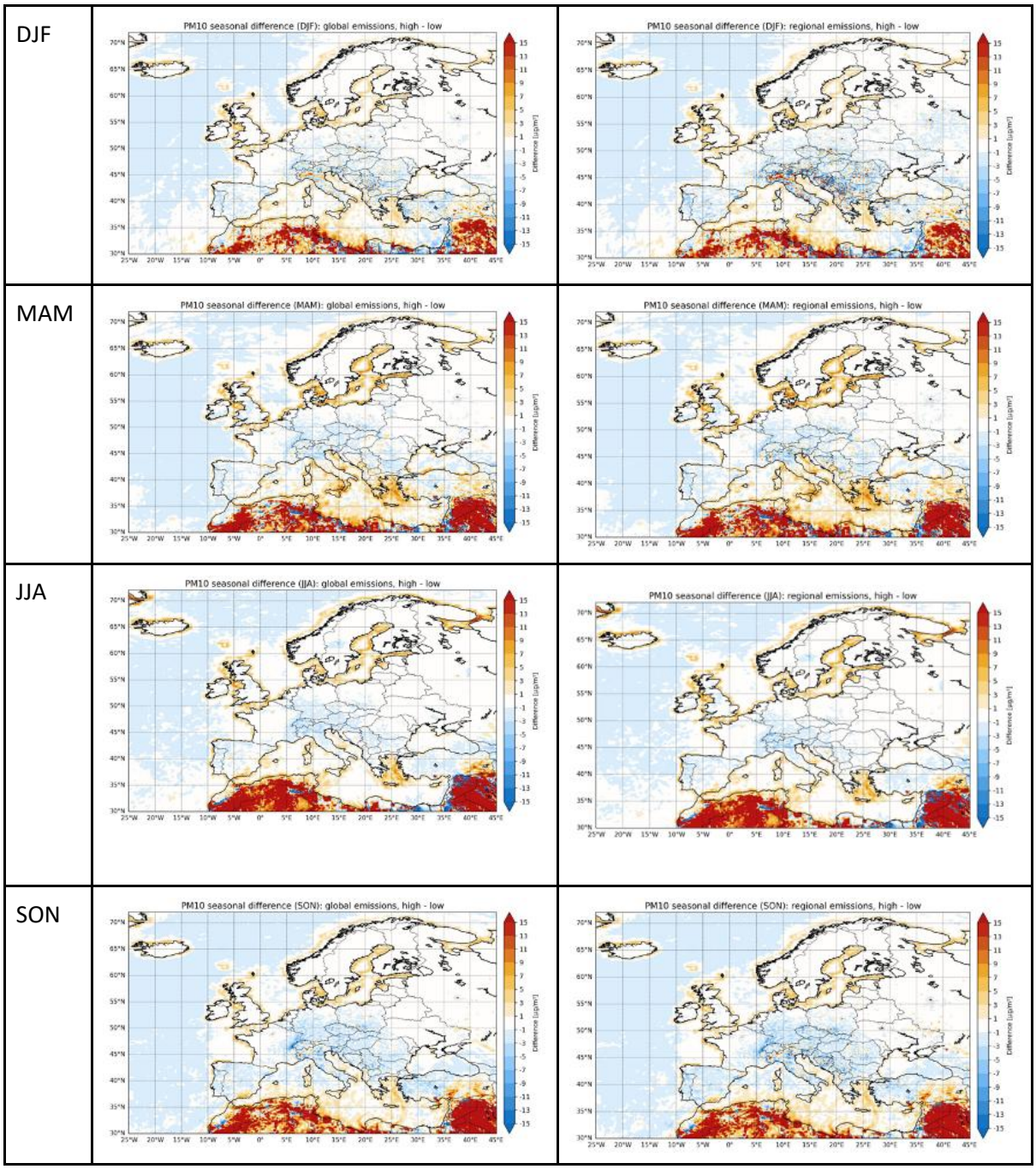

Figure 3.6. PM10 concentration delta between results obtained with high resolution simulation 0.1 deg and low resolution simulation 0.5 deg calculated with GLOB emission inventory (left panel) and REG emission inventory (right panel).

In the case of PM2.5, the main spatial and temporal characteristics of resolution-related differences are broadly similar to those observed for PM10. The spatial patterns of the annual and seasonal mean differences follow a comparable structure, with elevated concentrations in high-resolution simulations typically located over urban and industrial areas.

When comparing the annual average differences with the seasonal averages, it becomes evident that during the winter season (DJF), the positive differences between high- and low-resolution simulations are more widespread. These elevated values are not limited to the biggest urban hotspots but extend across a broader set of smaller cities and urbanized regions. This widespread enhancement in winter PM2.5 concentrations at high resolution may

reflect better representation of emissions from the residential sector, which are particularly significant during colder months. Since residential combustion, often for heating purposes, is both spatially heterogeneous and temperature-dependent, finer resolution enables a more localized and temporally responsive depiction of these sources.

In contrast to PM10, the differences over North Africa are smaller for PM2.5.

	GLOBAL	REGIONAL
Year	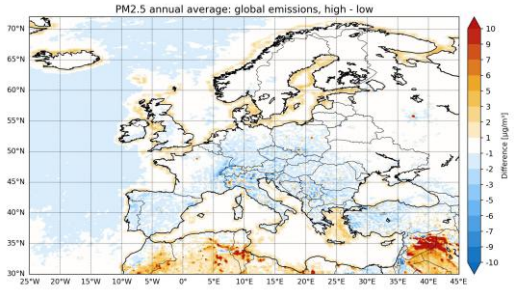	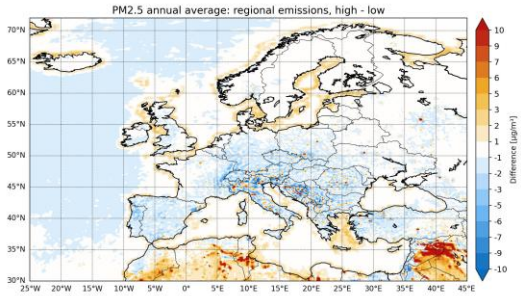
DJF	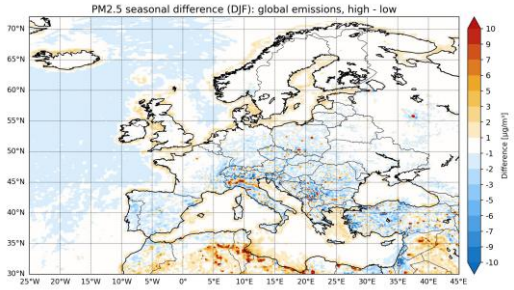	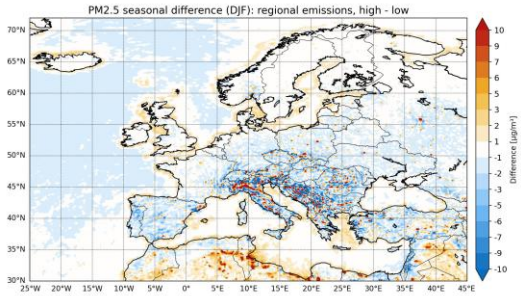
MAM	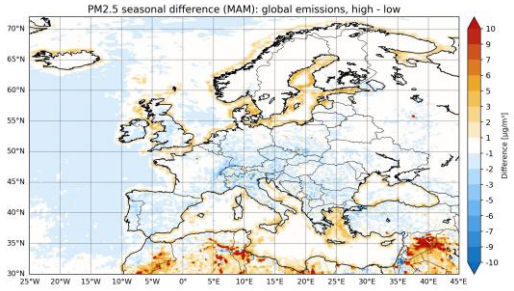	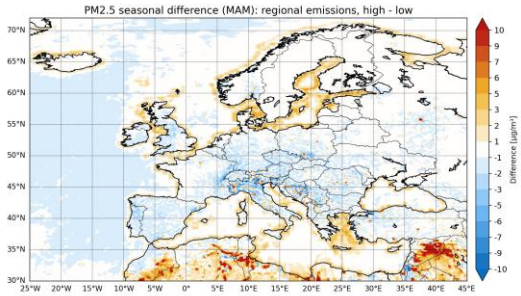

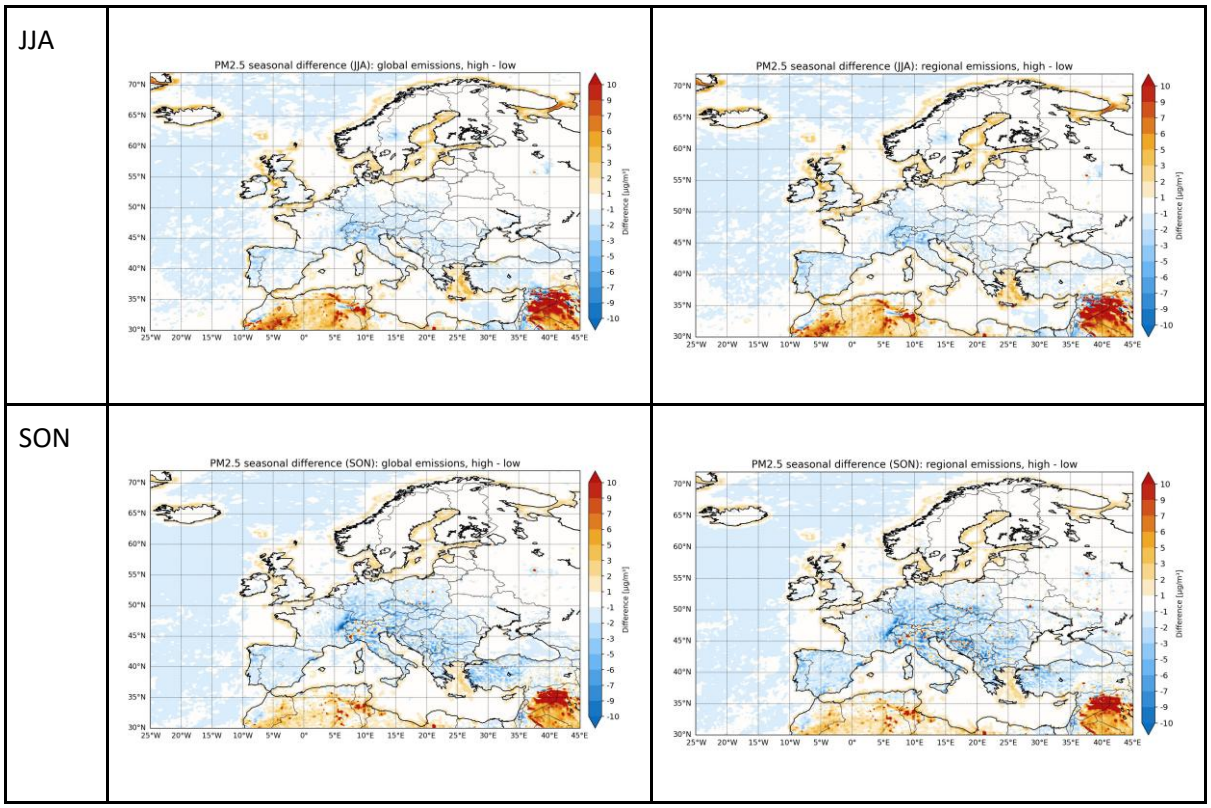

Figure 3.7. PM2.5 concentration delta between results obtained with high resolution simulation 0.1 deg and low resolution simulation 0.5 deg calculated with GLOB emission inventory (left panel) and REG emission inventory (right panel)

5.2.2.2 Daily concentration delta time series by regions

Daily time series analyses reveal additional insights into the differences between simulations conducted at higher (0.1 deg) and lower (0.5 deg) spatial resolution using the IFS-COMPO with both global and regional emission inventories.

Over the majority of the domain, simulations at higher resolution tend to produce lower daily concentrations compared to those at coarser resolution. These differences typically range from -1 to -5 µg/m³ and are clearly visible in the time series plots across most regions.

In addition to the general tendency for lower concentrations in high-resolution simulations, the daily time series reveal several short-term episodes where concentrations are significantly higher at high resolution compared to the coarse-resolution runs. These events appear as sharp peaks and are most likely associated with long-range pollutant transport.

In terms of regional behaviour, the temporal pattern of the difference between the two resolutions is quite consistent across the two emission inventories in several regions. For example, in Spain, France, and Iceland, the overall magnitude and timing of the differences are similar regardless of whether global or regional emissions are used. In contrast, the Po Valley region in northern Italy exhibits a higher amplitude of variability in the differences when regional emissions are used. Similarly, noticeable resolution-related differences are observed for Poland and Romania.

	GLOB	REG
Spain	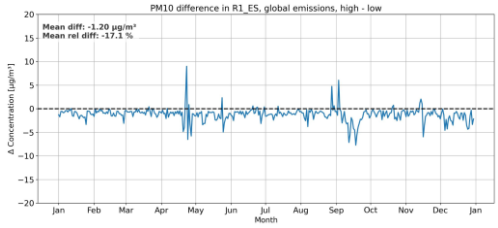	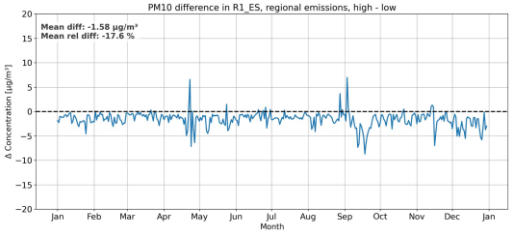
France	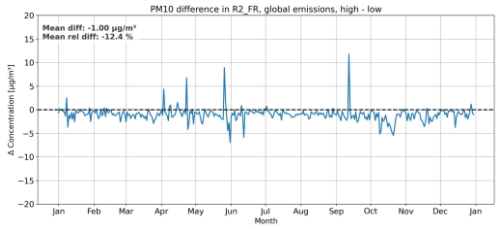	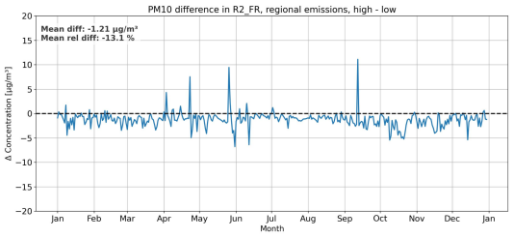
Italy	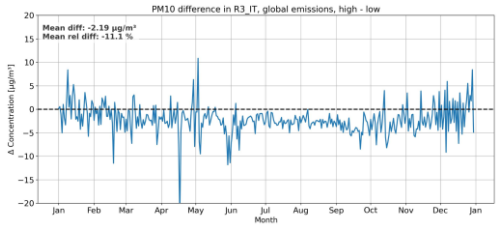	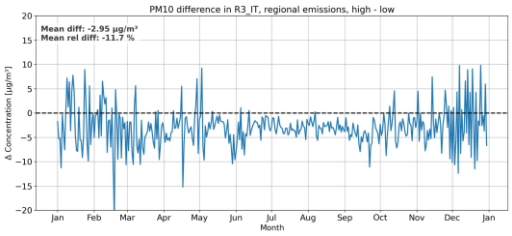
NL	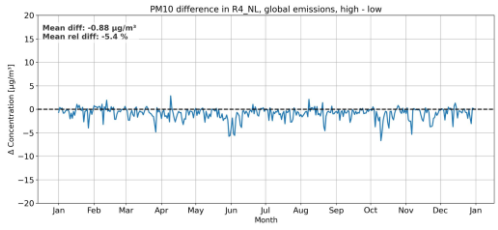	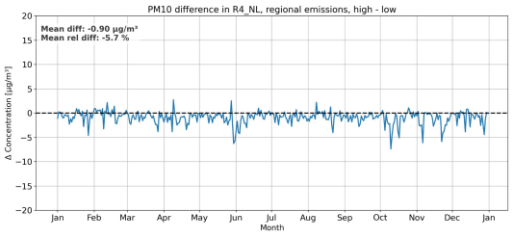
Poland	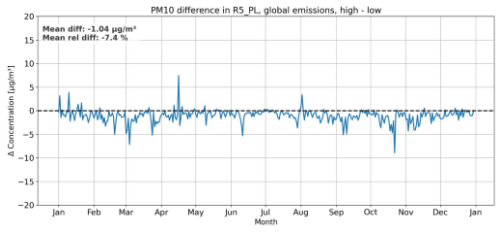	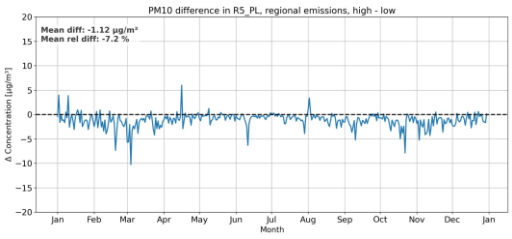
Romania	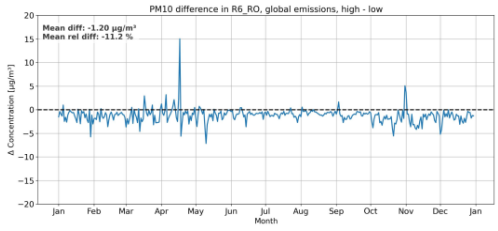	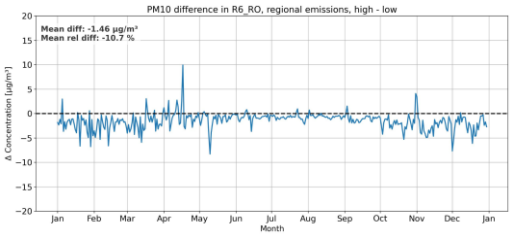

Iceland	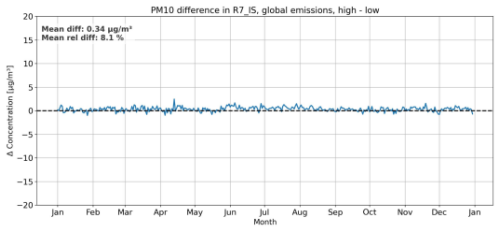	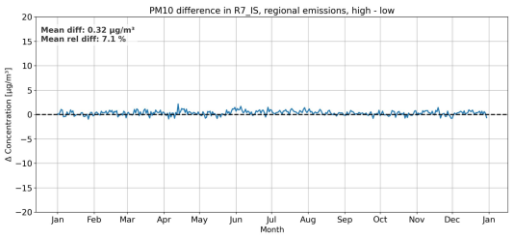

Figure 3.8. PM10 daily concentration delta obtained with high resolution 0.1 deg and low resolution 0.5 deg averaged over individual regions, calculated with GLOB emission inventory (left panel) and REG emission inventory (right panel)

	GLOB	REG
Spain	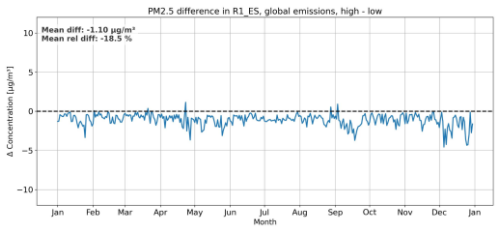	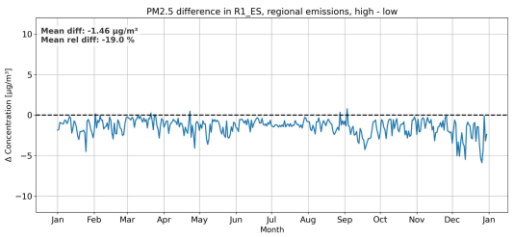
France	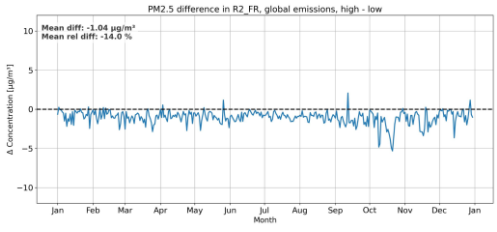	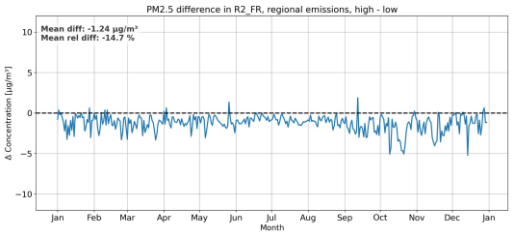
Italy	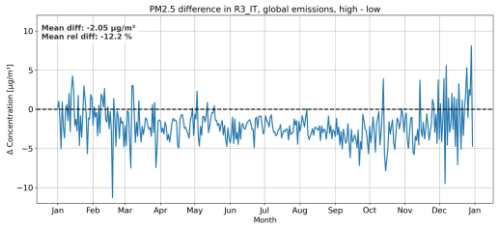	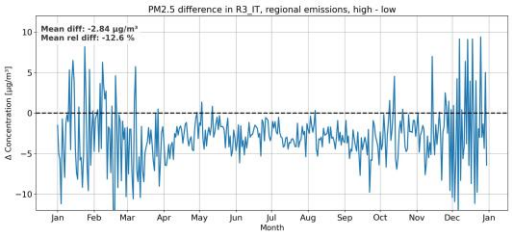
NL	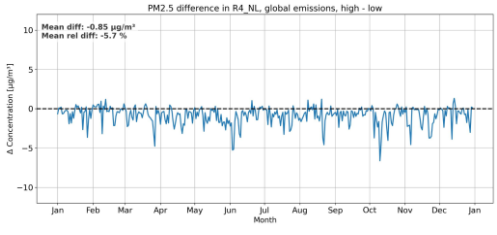	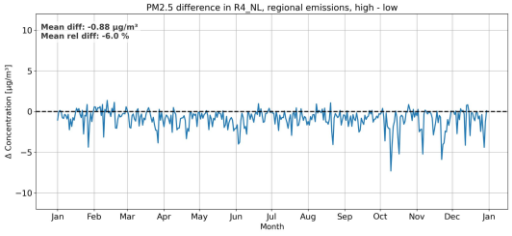

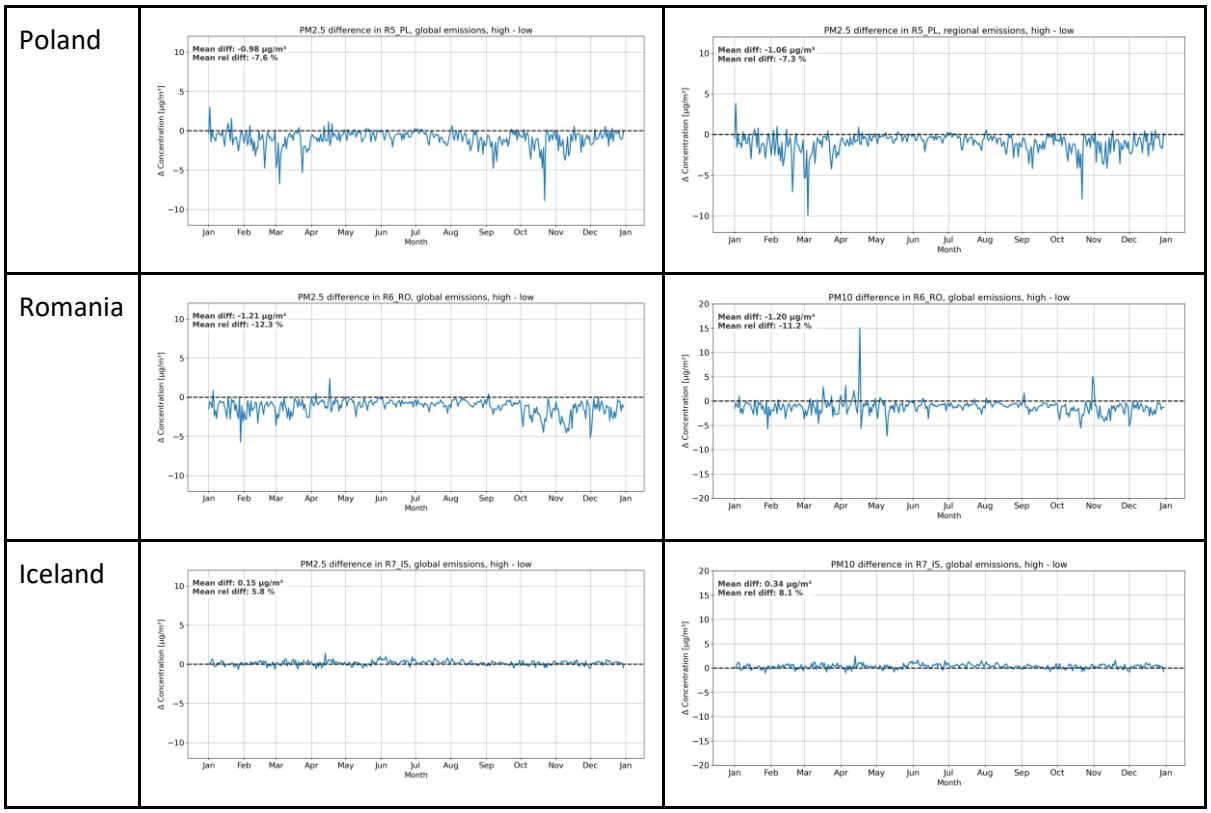

Figure 3.9. PM2.5 daily concentration delta obtained with high resolution 0.1 deg and low resolution 0.5 deg averaged over individual regions, calculated with GLOB emission inventory (left panel) and REG emission inventory (right panel)

5.3 Regional models intercomparison

This section presents intercomparison of the surface PM10 and PM2.5 concentrations as reproduced by eight regional models. Also, the regional models were compared to IFS-COMPO results obtained with the regional emission inventory at high resolution (0.1 deg).

5.3.1 Spatial differences

The intercomparison of PM10 and PM2.5 annual average concentrations and seasonal concentrations (maps in Appendix) was carried out for eight regional models: Chimere, DEHM, EMEP, GEM-Aq, Lotos EUROS, MINNI, MONARCH, SILAM).

Spatial distribution of annual PM10 and PM2.5 concentration fields varies noticeably across models. While the main hotspot regions—such as the Po Valley, Southern Poland, and parts of Romania—are consistently captured, the intensity and spatial extent of these high-concentration zones differ between models. These differences may be attributed to various factors, including differences in how secondary aerosol production is represented, assumptions about particle lifetime, and the treatment of removal processes such as dry and wet deposition. Furthermore, differences in vertical resolution and mixing depth could

influence the degree to which surface concentrations build up in stable atmospheric conditions, particularly during winter.

Noticeable differences in concentrations over the ocean and North Africa point to differences in the formulation of surface interaction processes and natural emissions. Over the ocean, these differences are likely related to how sea spray generation and dry deposition are represented, both of which depend on wind speed and humidity.

In North Africa, the variation is mainly driven by differences in the treatment of desert dust emissions, which are influenced by surface characteristics such as soil type and land cover, as well as wind conditions.

	PM10	PM2.5
IFS-COMPO HIGH REG	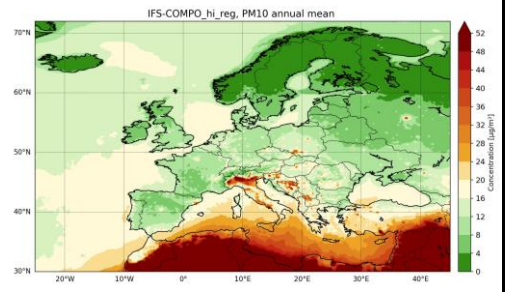	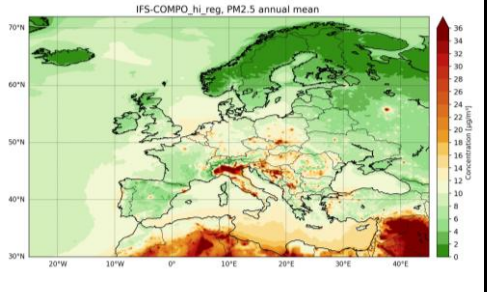
Chimere	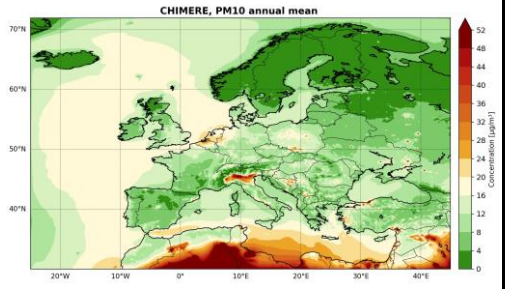	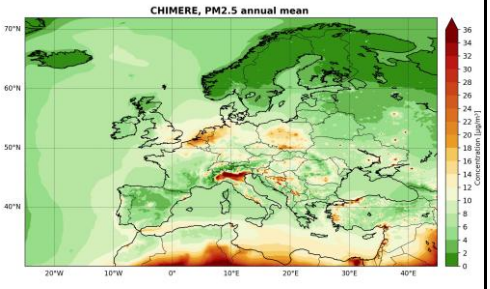
DEHM	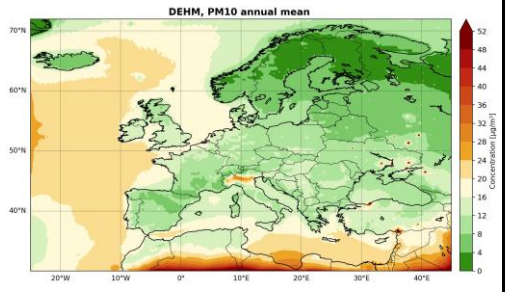	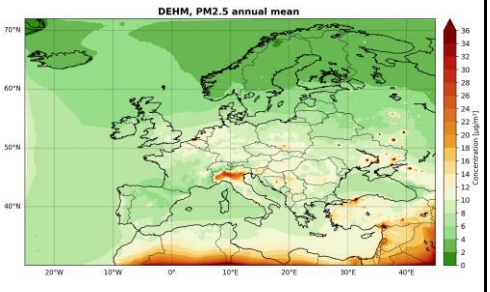
EMEP	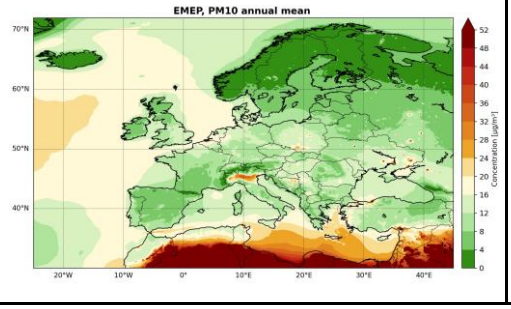	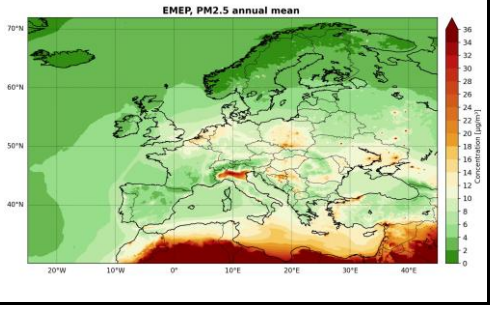

GEM-AQ	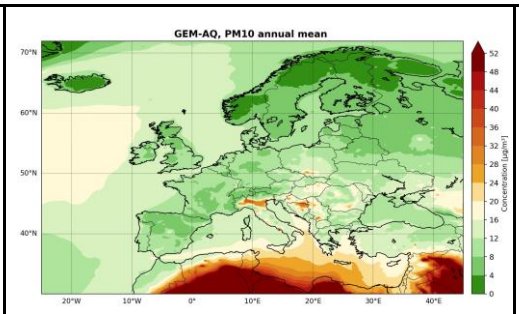	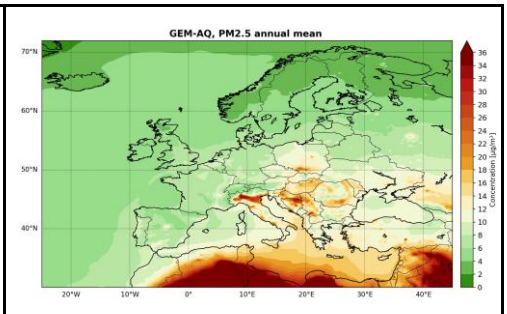
Lotos Euros	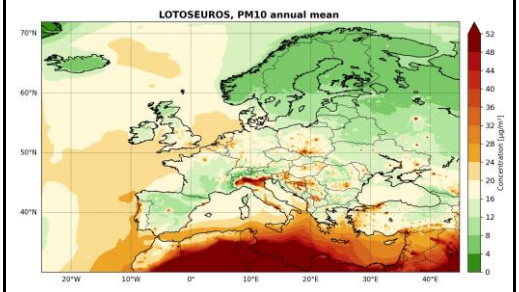	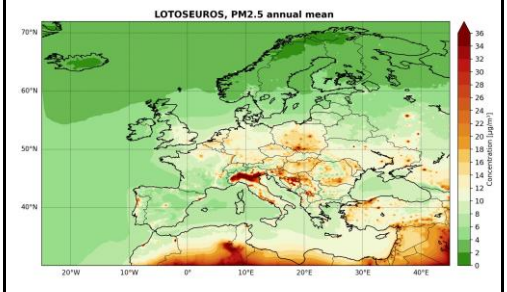
MINNI	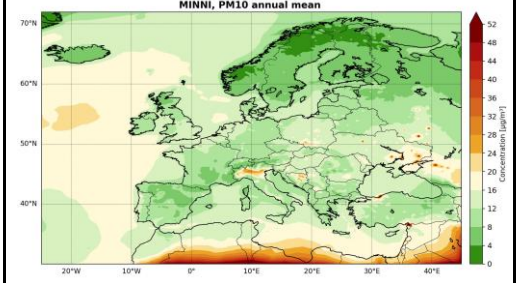	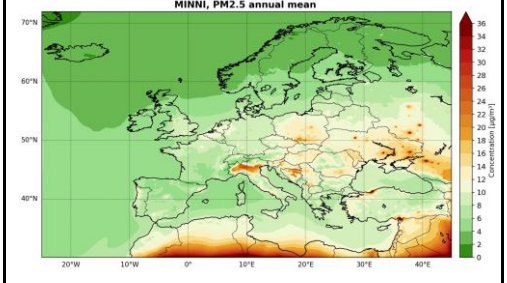
MONARCH	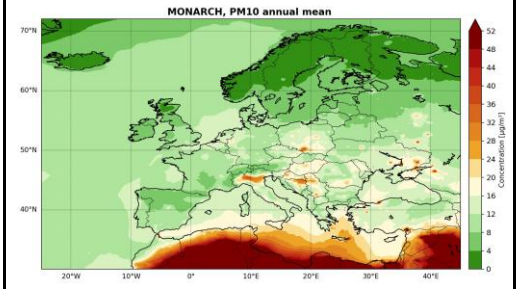	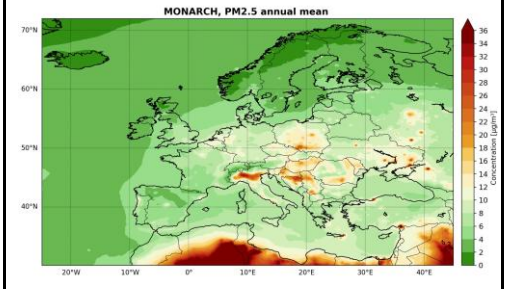
SILAM	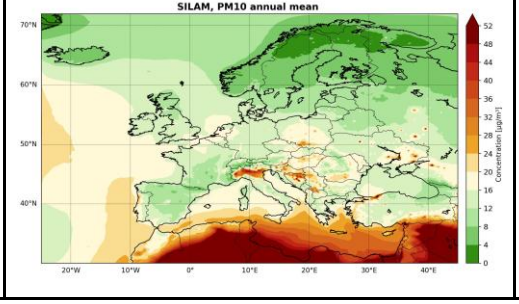	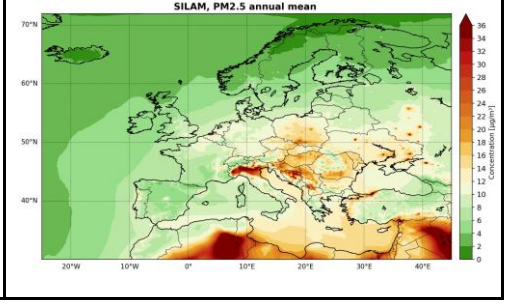

Figure 3.10 PM10 and PM2.5 annual averaged concentrations calculated with individual regional models

Histograms plotted based on the “over land” grid points illustrate the distribution of modelled annual average PM10 concentrations across all grid cells, comparing the results from individual regional models and the IFS-COMPO simulation at high resolution using regional emissions (HIGH-REG). For most regional models, the majority of grid cells fall within the 5–25 µg/m³ concentration range. However, a systematic difference is observed in the upper tail of the distribution. In particular, the IFS-COMPO HIGH-REG configuration yields a notably higher number of grid cells exceeding 40 µg/m³ compared to any of the regional models.

annual	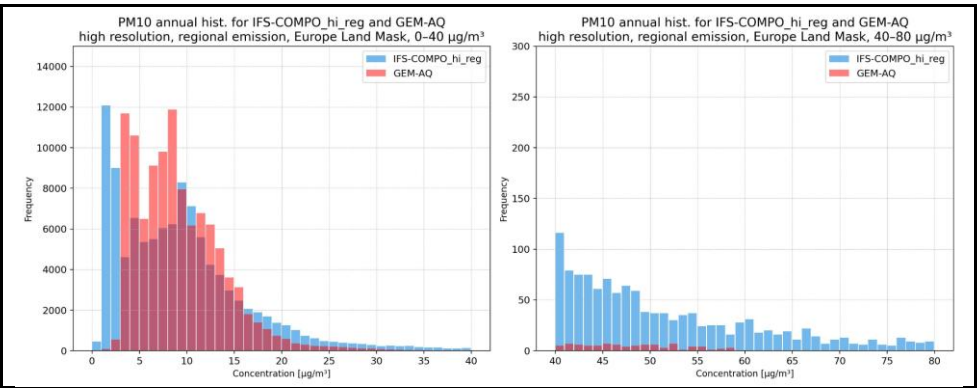
DJF	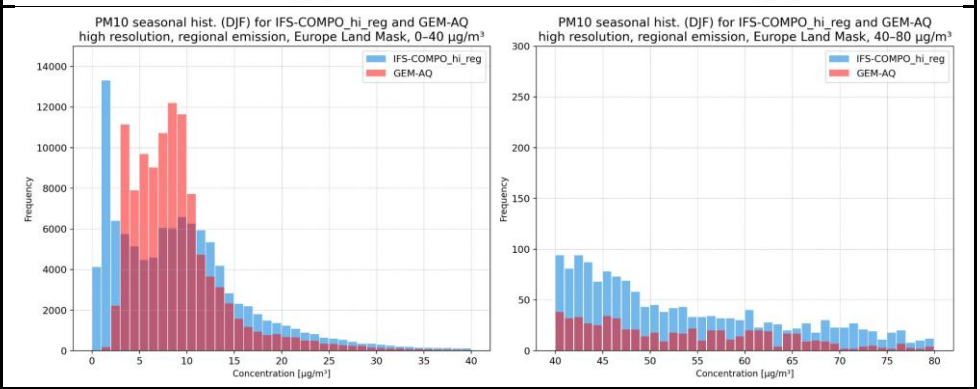
MAM	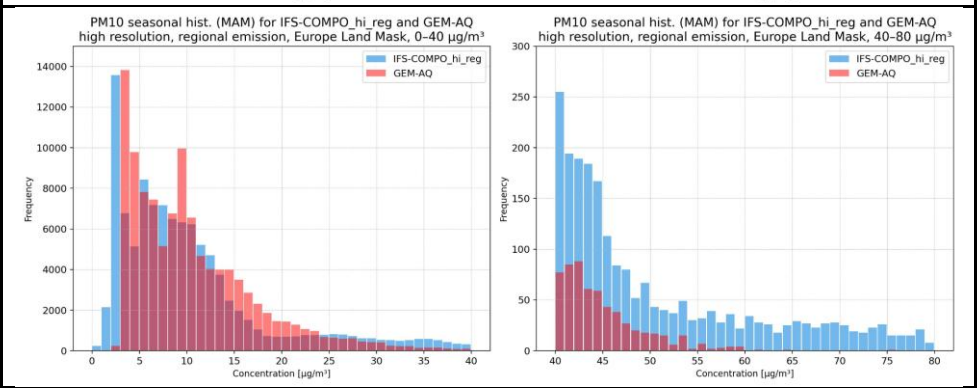
JJA	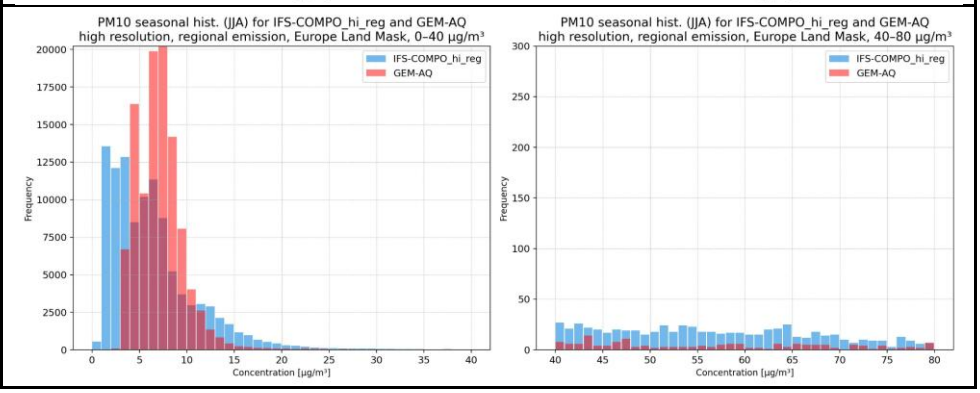

SON	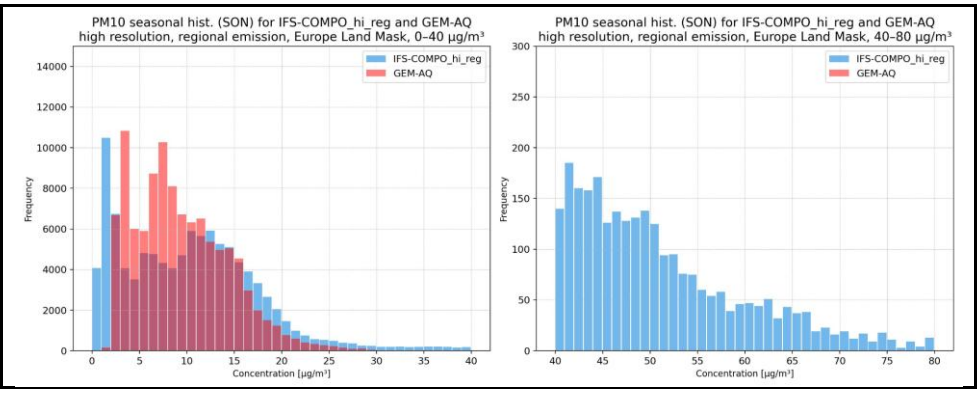

Figure 3.11 Example of histogram for the GEM-AQ and IFS Compo HIGH REG for the annual average and seasons

5.3.2 Regional Ensemble variability

To further deepen the comparative analysis between the regional models and the IFS-COMPO HIGH-REG simulation, a regional ENSEMBLE was constructed. Differences between the ENSEMBLE and IFS-COMPO HIGH-REG were then calculated for both annual and seasonal mean concentrations.

Notable differences were observed for PM10, particularly over the Atlantic Ocean. On average, the regional models simulated higher PM10 concentrations over marine areas compared to IFS-COMPO HIGH-REG, likely due to stronger sea salt contributions. In contrast, for PM2.5, the regional models generally produced lower concentrations over the same areas.

Despite using the same emission dataset (CAMS REG), substantial differences between the regional ENSEMBLE and the global high-resolution simulation were also observed over land across all seasons. These differences highlight the influence of other model components—such as transport processes, deposition schemes, and chemical mechanisms—on the simulated concentration fields, even under harmonized emissions.

	PM10	PM2.5
annual	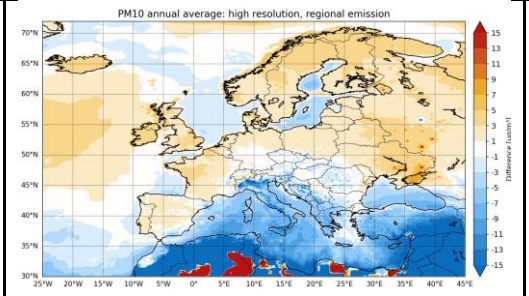	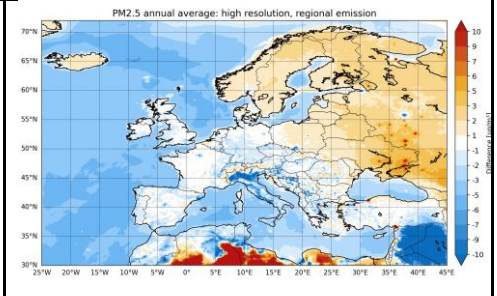
DJF	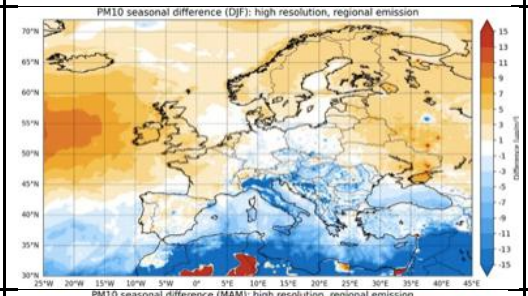	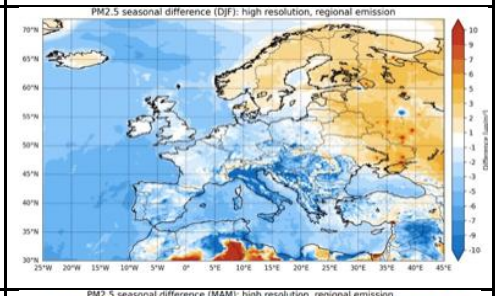
MAM	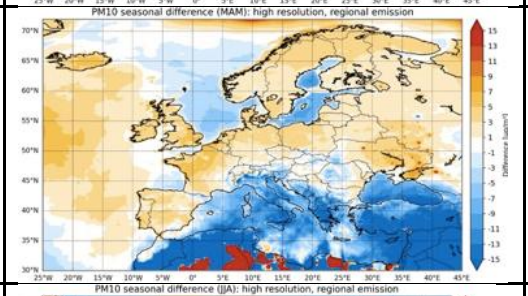	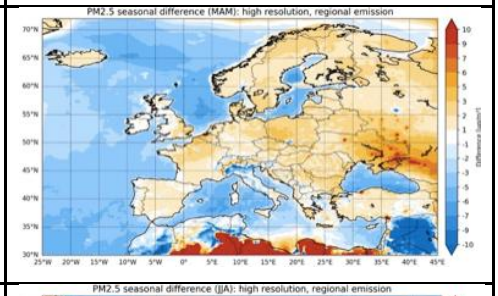
JJA	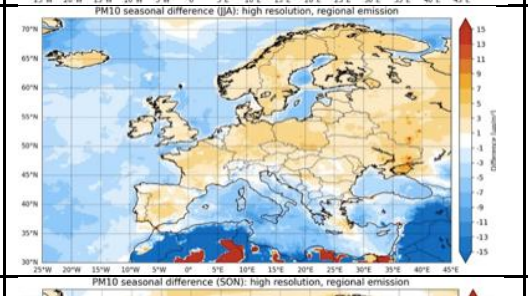	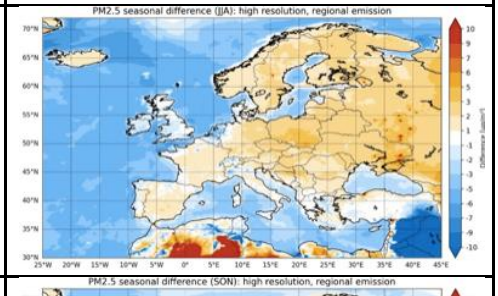
SON	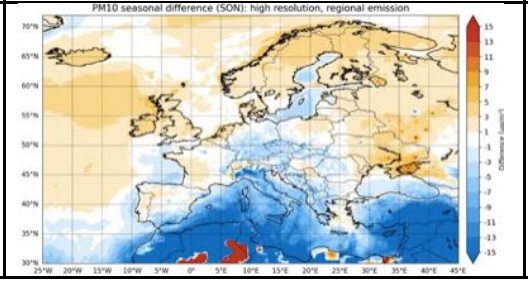	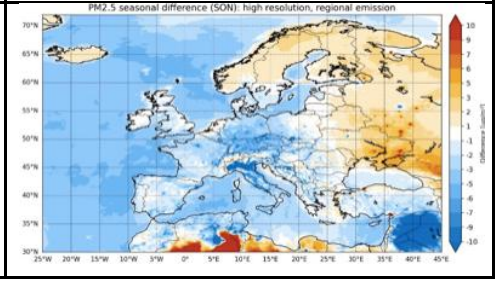

Figure 3.12 Differences between Ensemble and IFS COmpo HIGH REG as annual average and seasonal averages for PM10 and PM2.5

Based on the output of individual models, we assessed the temporal variability and spread of the ensemble across selected regions. The ensemble spread shows clear regional differences. In general, variability is higher in regions with complex emission patterns or strong seasonal signals, such as residential heating in winter. The highest variability tends to occur during peak pollution episodes, when differences between models become more pronounced. Conversely, in regions with lower emission levels, the ensemble spread remains relatively small throughout the year.

	PM10	PM2.5
Spain	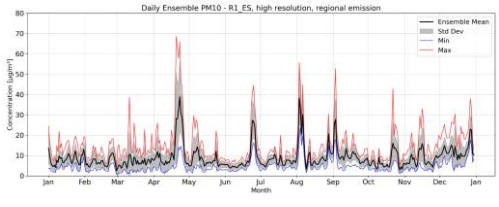	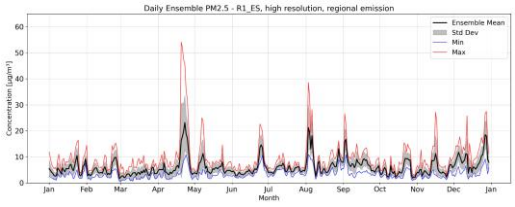
France	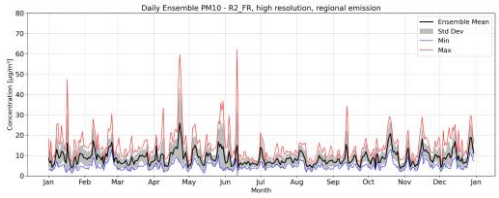	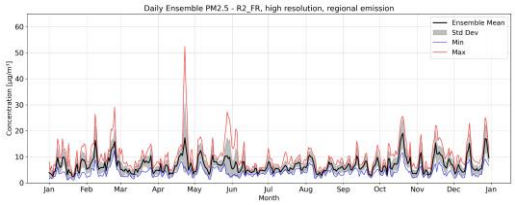
Italy	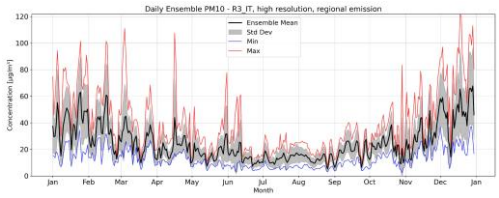	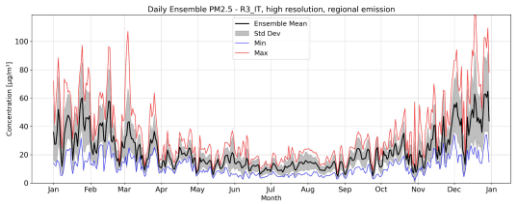
NL	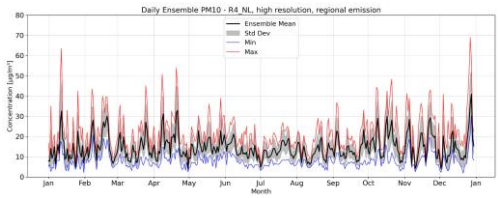	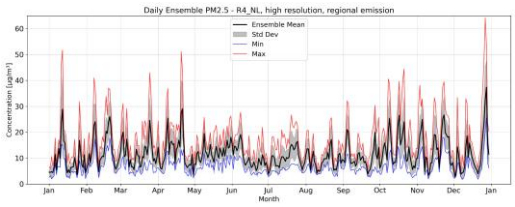
Poland	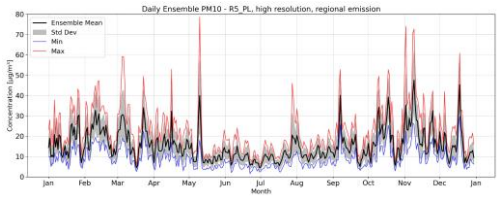	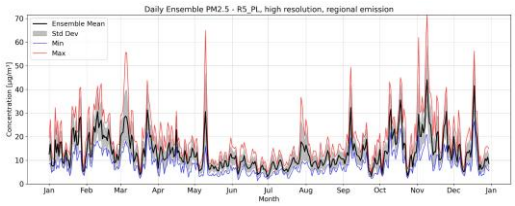
Romania	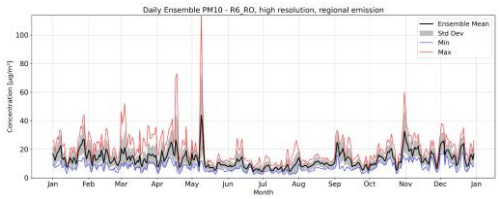	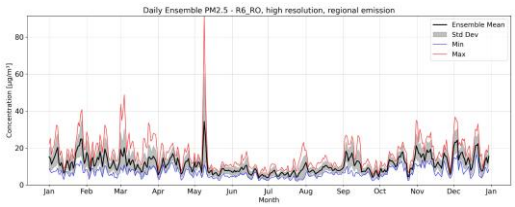
Iceland	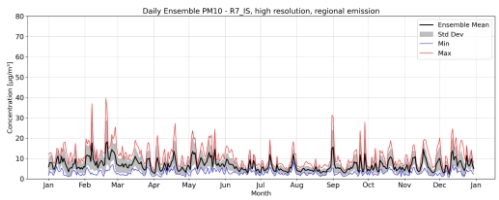	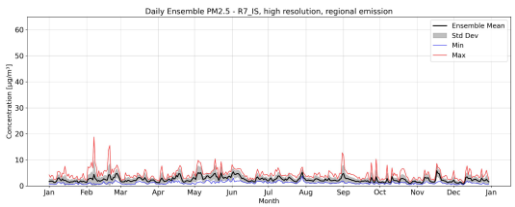

Figure 3.13 Regional Ensemble – time series for PM10 and PM2.5

5.3.3 Regional ensemble spread

To assess the variability between regional models, the standard deviation of the ensemble was calculated for both annual and seasonal mean concentrations. The highest values appear over North Africa, the Atlantic Ocean, and locally over urban and industrial hotspots.

Over the Atlantic, the elevated standard deviation is likely linked to differences in sea salt uptake between models. Over land, the variability is most noticeable in regions with high emissions, such as large urban areas or industrial zones, where differences in modelled emissions and processing lead to a wider spread.

In the northern part of the domain, the reason for increased standard deviation is less clear, especially since all regional models use the same boundary conditions. It may reflect model-specific sensitivities or numerical treatment near the domain edge.

	PM10	PM2.5
annual	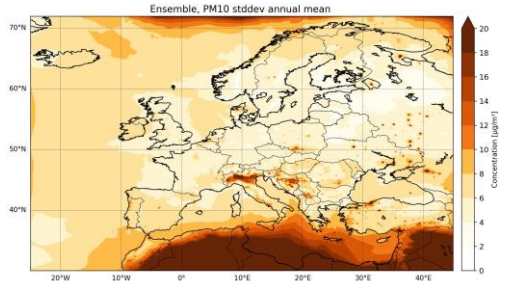	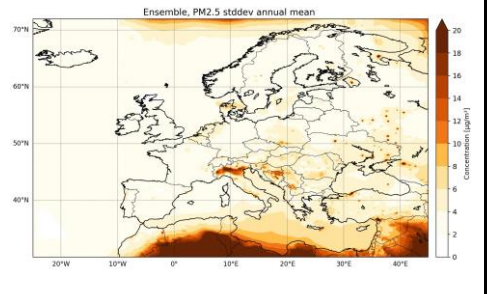
DJF	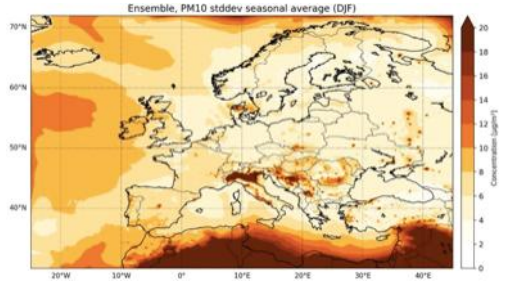	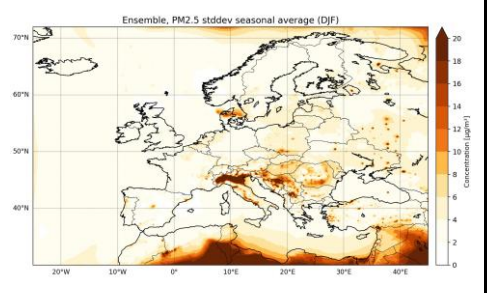
MAM	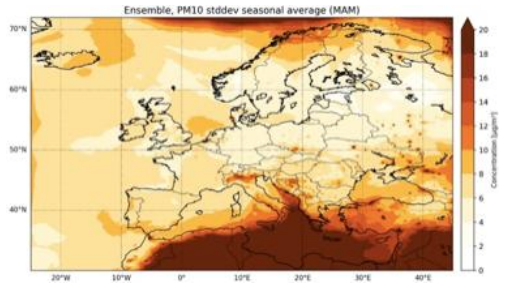	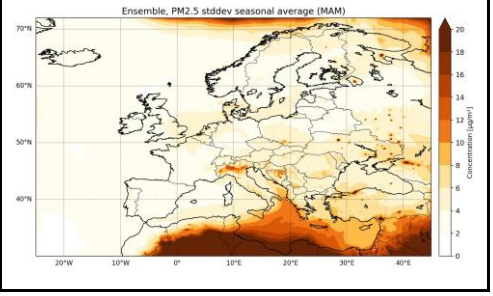

JJA	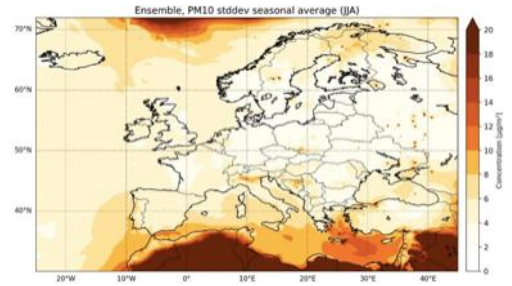	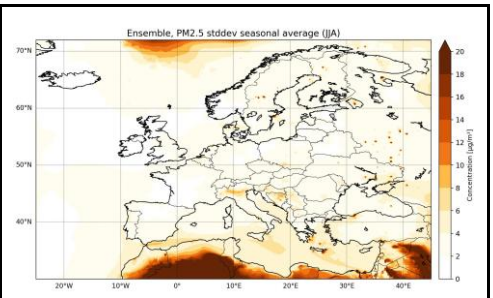
SON	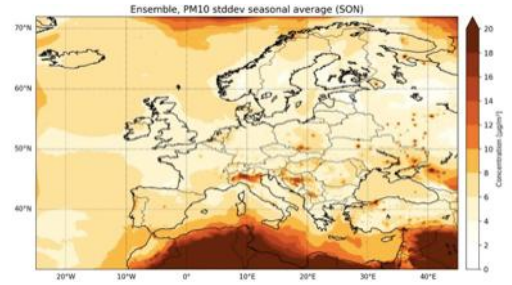	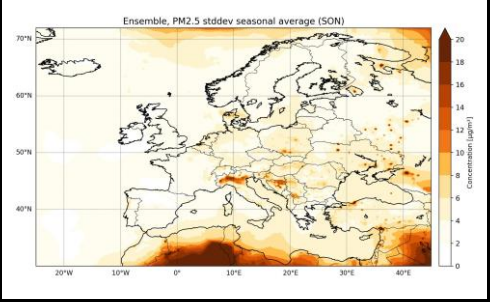

Figure 3.14 Standard deviation of the regional models based on annual and seasonal values for PM10 and PM2.5

5.4 Evaluation

Although model evaluation is not the main focus of this report, commenting on the agreement with observations remains important. The primary goal of atmospheric chemistry model development is to understand processes and causal relationships, but the correctness of the representation of these processes is ultimately assessed through error analysis.

The following statistical measures were calculated: mean bias, indicating the model's tendency to systematically overestimate or underestimate concentrations; root mean square error (RMSE), representing the total error; and the Pearson correlation coefficient, indicating how well the temporal variability is captured. These metrics were calculated for each participating model and for each selected region.

The results, presented in the table below, show that model performance is both region- and season-dependent.

In Western Europe—specifically Spain, France, and the Netherlands—there is a tendency for models to overestimate PM10 concentrations, particularly during the colder months. In contrast, for Poland and Romania, models generally underestimate concentrations throughout the year. This underestimation may not be directly related to national emission inventories, as long-range transport contributes 40–50% of annual average concentrations in these regions. Instead, it could reflect the challenge in accurately representing stable atmospheric conditions typical for areas with continental or transitional climates.

During summer, PM10 concentrations in Spain tend to be underestimated. In the Po Valley, overestimation is observed consistently throughout the year.

For RMSE, the largest discrepancies were observed in the Po Valley, Poland, and Romania, reflecting greater challenges in accurately simulating concentrations in these areas, likely due to a combination of emission complexity and meteorological conditions.

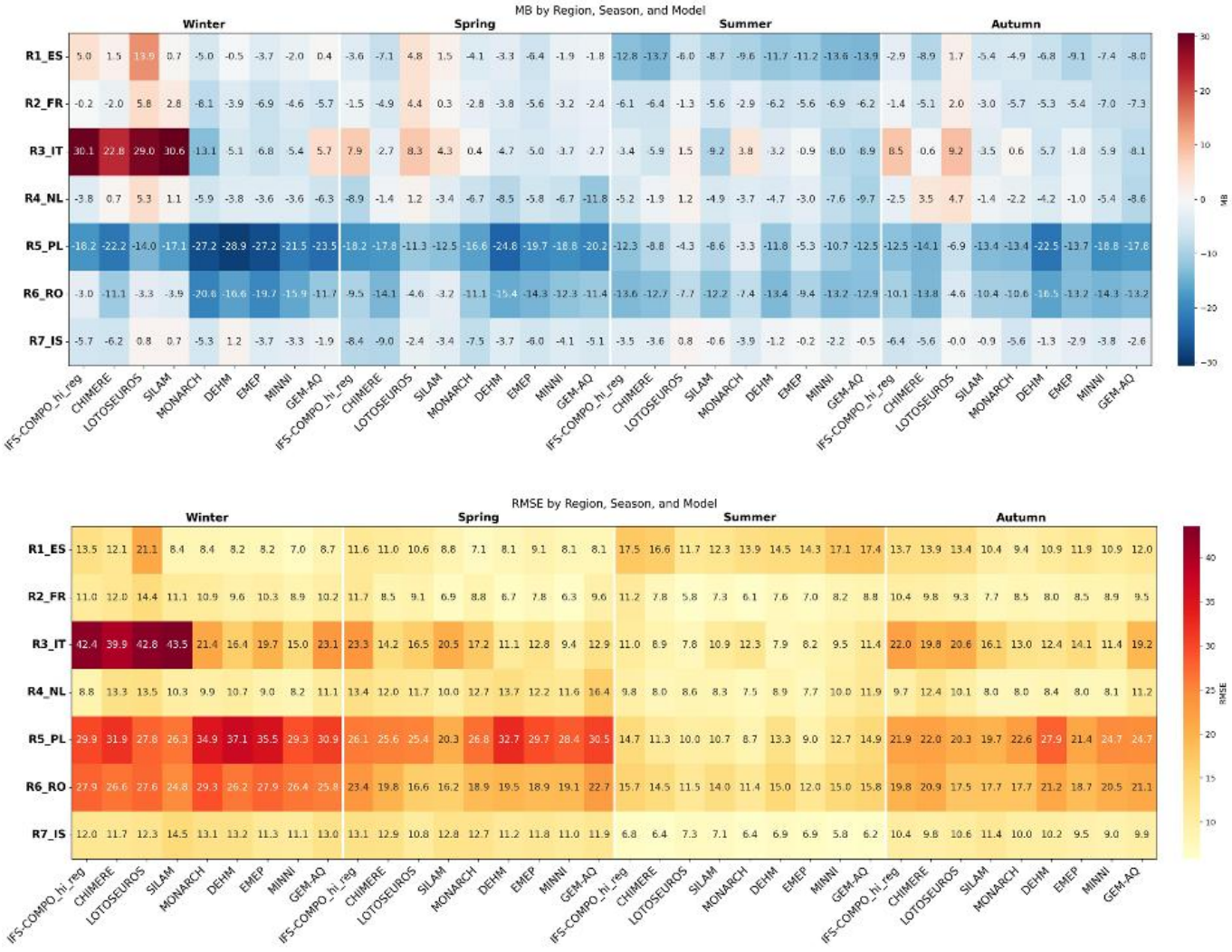

Figure 3.15 Mean bias (MB, top) and RMSE (bottom) of simulated PM10 for each region, model and season.

To highlight the differences between IFS-COMPO with regional emissions in the high-resolution setup and the ensemble of regional models, a comparison of error metrics was performed.

For PM10, the performance of IFS-COMPO HIGH-REG is generally comparable to that of the regional models across all regions. The error statistics—such as bias, RMSE, and correlation—tend to follow a consistent seasonal pattern, with similar magnitudes and variability over the year. This suggests that, despite differences in model formulation and resolution, the representation of PM10 is reasonably aligned across modeling systems.

In contrast, for PM2.5, the discrepancies between IFS-COMPO and the regional models are more pronounced.

	PM10	PM2.5
Spain	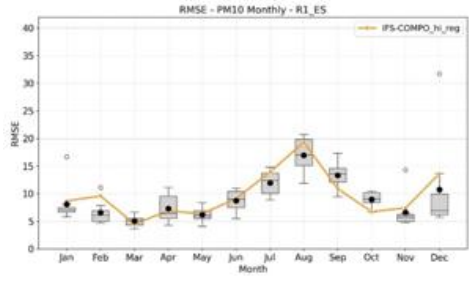	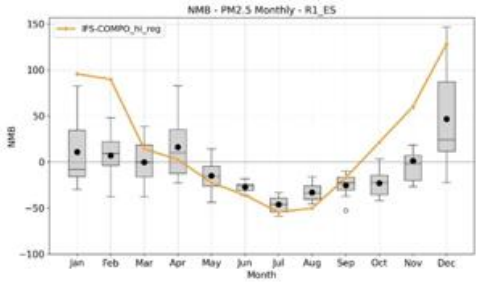
France		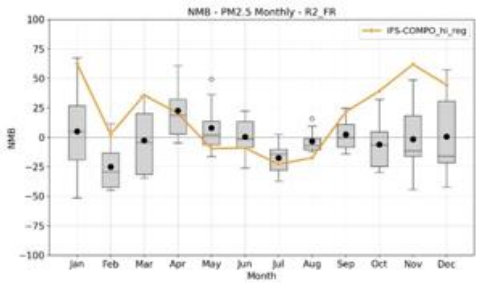
Italy	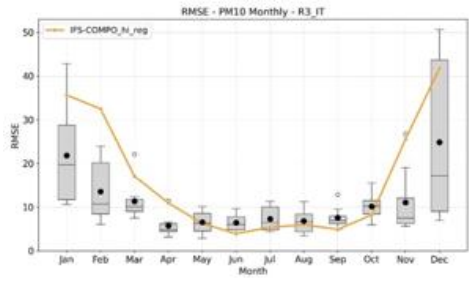	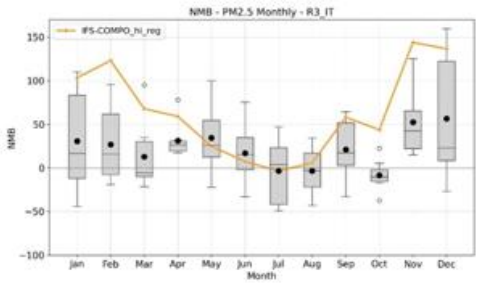
NL	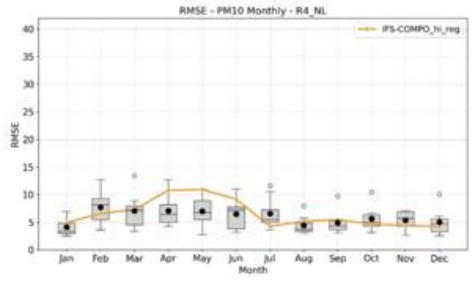	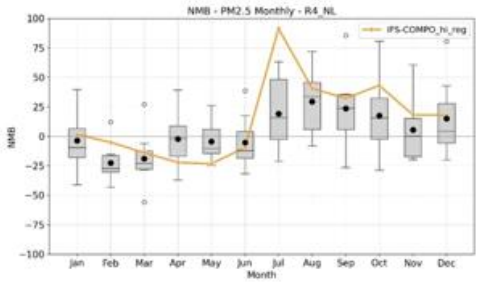
Poland	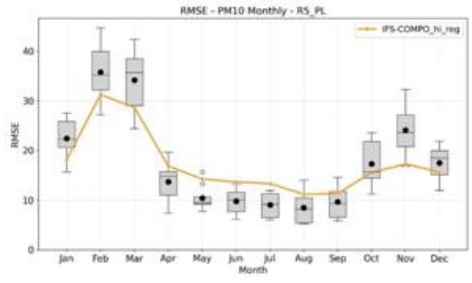	

Romania		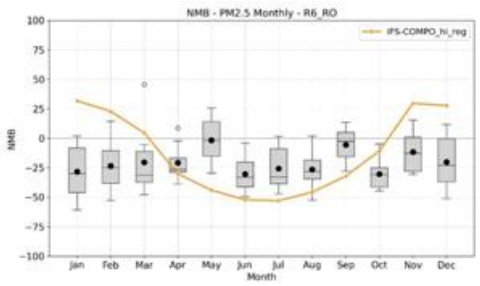
Iceland	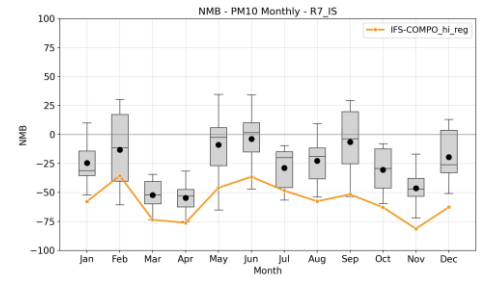	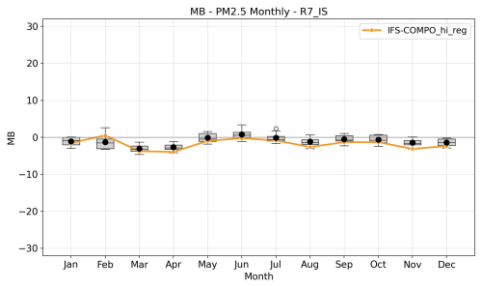

Figure 3.16 Monthly MB for IFC COMPO (HIGH REG) and ensemble PM10 and PM2.5, by region

Finally, Q–Q plots were produced to identify the concentration ranges where model performance deviates from observations, analysed per region and per model.

For Spain, all models tend to overestimate PM2.5 concentrations above 10 µg/m³. In the case of PM10, the situation is more varied—several models systematically underestimate concentrations across the full range, indicating a potential underrepresentation of coarse particle sources or removal processes. In France, model performance for PM10 and PM2.5 is relatively consistent. Models that underestimate PM10 tend to underestimate PM2.5 as well, and similarly for those that overestimate. This suggests coherent model behaviour in terms of aerosol treatment across size fractions. In the Netherlands, most models underestimate concentrations, particularly for values above 30 µg/m³. This underprediction at higher concentration levels points to potential difficulties in capturing peak pollution events. The Po Valley), models tend to overestimate concentrations up to around 40 µg/m³. Four models show especially strong overestimation. In Poland, all models consistently underestimate both PM10 and PM2.5, across nearly the entire concentration range. For Romania, a similar pattern is observed, with the majority of models underestimating observed concentrations, though with slightly more variation across models.

	PM10	PM2.5
Spain	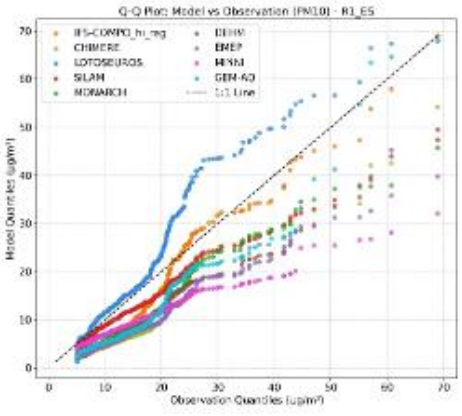	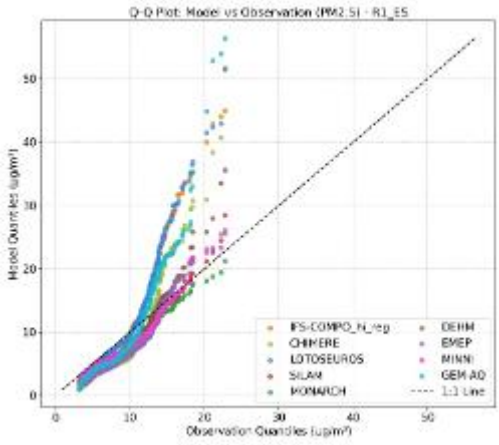

France	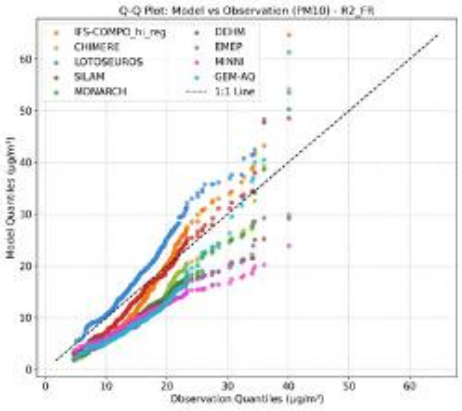	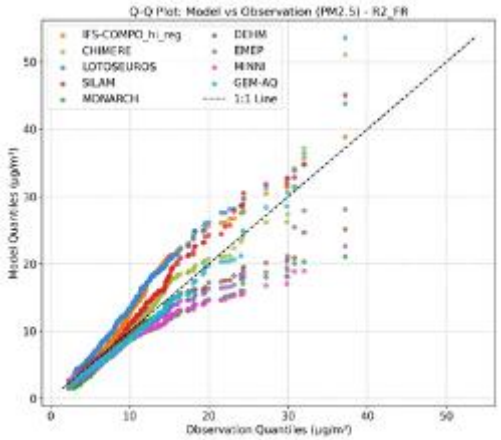
NL	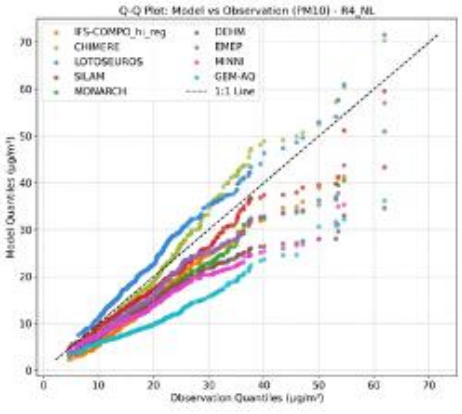	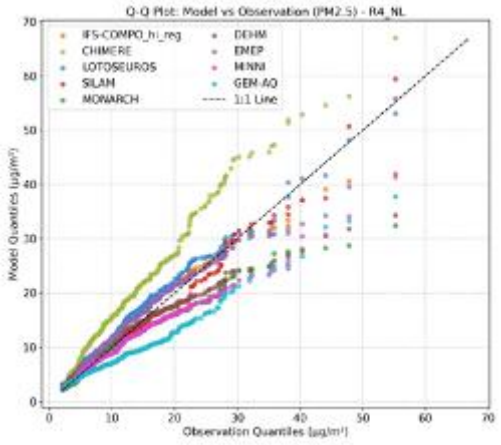
Italy	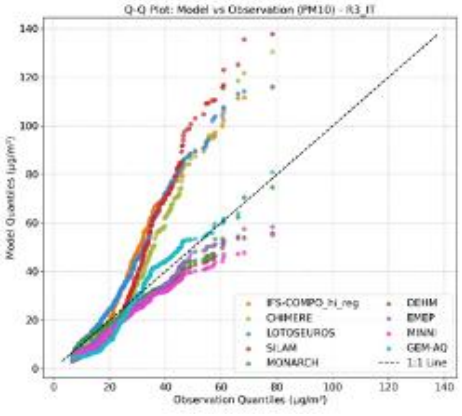	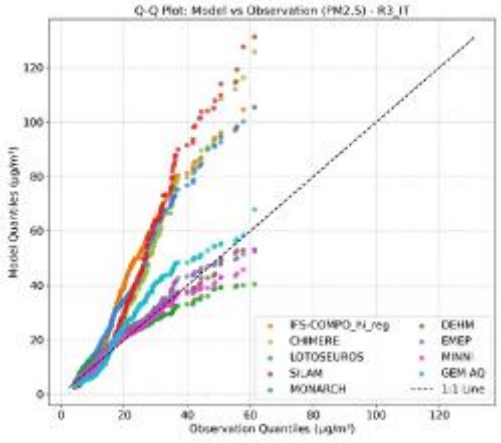

Poland	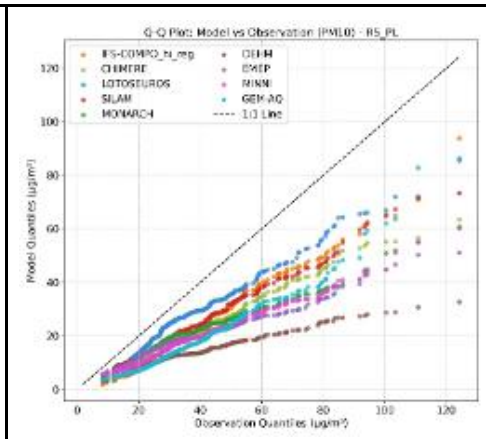	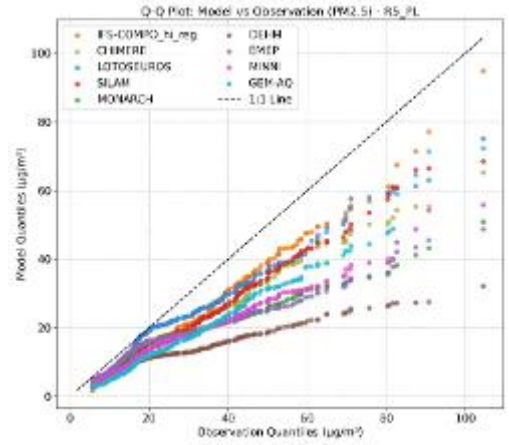
Romania	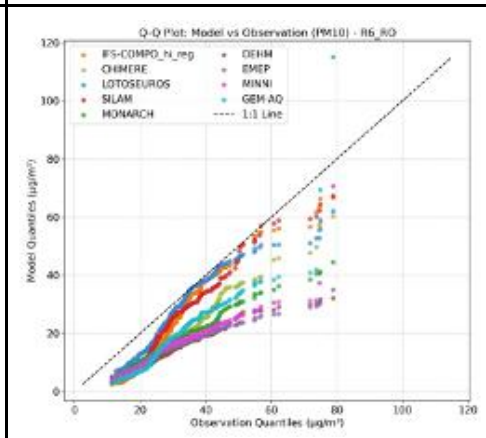	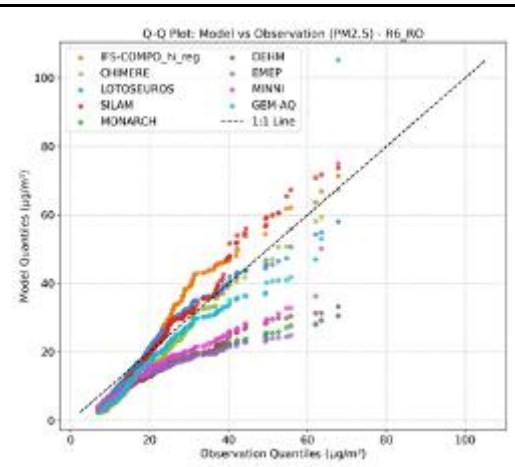
Iceland	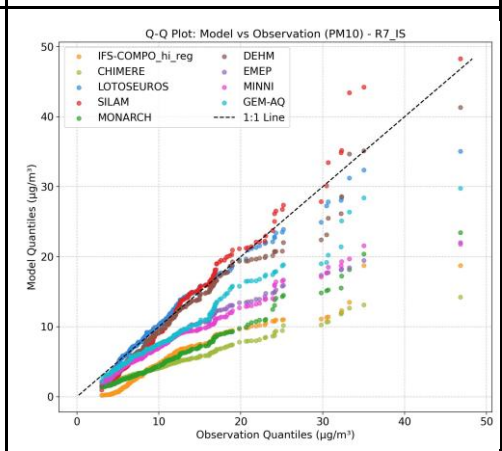	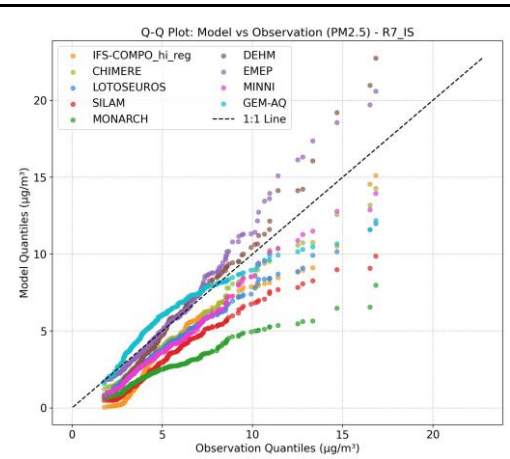

Figure 3.17 Q-Q plots for PM10 and PM2.5 based on the regional models and IFS-COMPO, by regions

Conclusion

The comparison involved global IFS-COMPO model configurations and an ensemble of eight regional European models,

The analysis highlights the sensitivity of IFS-COMPO simulations to both the choice of emission inventory and model resolution. Using regional emissions consistently results in higher pollutant concentrations over known anthropogenic hotspots, especially during winter months. This pattern is particularly evident for PM2.5 due to the role of residential heating and the longer atmospheric lifetime of fine particles, and also from the fact that condensables are included in the regional emissions and not in the global ones. In contrast, areas with low anthropogenic influence, such as Northern Europe and open ocean regions, show minimal differences, suggesting that emissions, rather than natural sources, drive most variability.

Resolution also plays an important role, with higher-resolution simulations producing sharper spatial gradients—higher concentrations in hotspots and lower levels in remote areas. Differences over oceans and coastal regions are likely related to how sea spray and surface interactions are represented. Time series analysis reveals that high-resolution runs generally produce slightly lower average concentrations, but also capture episodic pollution events more clearly.

A comparison with regional models shows that, despite using the same emissions, significant differences persist. The IFS-COMPO high-resolution configuration tends to reproduce more high-concentration grid cells than regional models, particularly above 40 µg/m³. Ensemble spread varies by region and is largest in areas with complex emissions or strong seasonal signals, such as winter heating. Over the Atlantic Ocean, regional models tend to show higher PM10 due to stronger sea salt uptake, while for PM2.5, concentrations are generally lower than in IFS-COMPO. In North Africa, regional models typically simulate higher PM concentrations, likely linked to differences in wind fields and surface representation that affect desert dust emissions.

Model evaluation against observations reveals region- and season-dependent biases. In Western Europe, models often overestimate PM levels in colder months, while in Eastern Europe, concentrations are generally underestimated.

Document History

Version	Author(s)	Date	Changes
1.0	Rose-Cloé Meyer, Samuel Remy, Joanna Strużewska, Jacek Kaminski	27/06/2025	Initial version

Internal Review History

Internal Reviewers	Date	Comments